

MTH1 deficiency selectively increases non-cytotoxic oxidative DNA damage in lung cancer cells: more bad news than good?

--Manuscript Draft--

Manuscript Number:	BCAN-D-17-01224R3
Full Title:	MTH1 deficiency selectively increases non-cytotoxic oxidative DNA damage in lung cancer cells: more bad news than good?
Article Type:	Research article
Section/Category:	Cell and molecular biology
Funding Information:	
Abstract:	<p>Background: Targeted therapies are based on exploiting cancer-cell-specific genetic features or phenotypic traits to selectively kill cancer cells while leaving normal cells unaffected. Oxidative stress is a cancer hallmark phenotype. Given that free nucleotide pools are particularly vulnerable to oxidation, the nucleotide pool sanitising enzyme, MTH1, is potentially conditionally essential in cancer cells. However, findings from previous MTH1 studies have been contradictory, meaning the relevance of MTH1 in cancer is still to be determined. Here we ascertained the role of MTH1 specifically in lung cancer cell maintenance, and the potential of MTH1 inhibition as a targeted therapy strategy to improve lung cancer treatments.</p> <p>Methods: Using siRNA-mediated knockdown or small-molecule inhibition, we tested the genotoxic and cytotoxic effects of MTH1 deficiency on H23 (p53-mutated), H522 (p53-mutated) and A549 (wildtype p53) non-small cell lung cancer cell lines relative to normal MRC-5 lung fibroblasts. We also assessed if MTH1 inhibition augments current therapies.</p> <p>Results: MTH1 knockdown increased levels of oxidatively damaged DNA and DNA damage signaling alterations in all lung cancer cell lines but not normal fibroblasts, despite no detectable differences in reactive oxygen species levels between any cell lines. Furthermore, MTH1 knockdown reduced H23 cell proliferation. However, unexpectedly, it did not induce apoptosis in any cell line or enhance the effects of gemcitabine, cisplatin or radiation in combination treatments. Contrastingly, TH287 and TH588 MTH1 inhibitors induced apoptosis in H23 and H522 cells, but only increased oxidative DNA damage levels in H23, indicating that they kill cells independently of DNA oxidation and seemingly via MTH1-distinct mechanisms.</p> <p>Conclusions: MTH1 has a NSCLC-specific p53-independent role for suppressing DNA oxidation and genomic instability, though surprisingly the basis of this may not be reactive-oxygen-species-associated oxidative stress. Despite this, overall our cell viability data indicates that targeting MTH1 will likely not be an across-the-board effective NSCLC therapeutic strategy; rather it induces non-cytotoxic DNA damage that could promote cancer heterogeneity and evolution.</p>
Corresponding Author:	Steven S Foster, Ph.D. University of Leicester College of Medicine Biological Sciences and Psychology Leicester, Leicestershire UNITED KINGDOM
Corresponding Author Secondary Information:	
Corresponding Author's Institution:	University of Leicester College of Medicine Biological Sciences and Psychology
Corresponding Author's Secondary Institution:	
First Author:	Steven S. Foster, Ph.D.
First Author Secondary Information:	
Order of Authors:	Steven S. Foster, Ph.D.

	George D.D. Jones, Ph.D.
	Mark D. Evans, Ph.D.
	Kheloud M.H. Alhamoudi, B.Sc.
	Hussein H.K. Abbas
Order of Authors Secondary Information:	
Response to Reviewers:	The authors' response letter has been included as a supplementary file

[Click here to view linked References](#)

1 **MTH1 deficiency selectively increases non-cytotoxic oxidative DNA damage in lung cancer cells:**

2 **more bad news than good?**

3

4 Hussein H.K. Abbas^{1,2}, Kheloud M.H. Alhamoudi¹, Mark D. Evans³, George D.D. Jones^{1‡} and Steven S.

5 Foster^{1*}

6

7 *Corresponding author: ssf5@le.ac.uk

8 ‡Correspondence may also be addressed to: gdj2@le.ac.uk

9 ¹Department of Genetics and Genome Biology, University of Leicester, Leicester, Leicestershire, LE1

10 7RH, UK

11

12 **Author details**

13 ¹Department of Genetics and Genome Biology, University of Leicester, Leicester, Leicestershire, LE1

14 7RH, UK.

15 ²Department of Pathology and Forensic Medicine, College of Medicine, Al-Mustansiriya University,

16 Baghdad, Iraq.

17 ³Faculty of Health and Life Sciences, De Montfort University, Leicester, Leicestershire, LE1 9BH,

18 England.

19 Other author's email addresses: H.H.K.A.: hhka1@le.ac.uk; K.M.H.A.: kmha2@le.ac.uk; M.D.E.:

20 mark.evans@dmu.ac.uk.

21

22

23

24

25

26

27 **Abstract**

28 **Background:** Targeted therapies are based on exploiting cancer-cell-specific genetic features or
29 phenotypic traits to selectively kill cancer cells while leaving normal cells unaffected. Oxidative stress
30 is a cancer hallmark phenotype. Given that free nucleotide pools are particularly vulnerable to
31 oxidation, the nucleotide pool sanitising enzyme, MTH1, is potentially conditionally essential in
32 cancer cells. However, findings from previous MTH1 studies have been contradictory, meaning the
33 relevance of MTH1 in cancer is still to be determined. Here we ascertained the role of MTH1
34 specifically in lung cancer cell maintenance, and the potential of MTH1 inhibition as a targeted
35 therapy strategy to improve lung cancer treatments.

36 **Methods:** Using siRNA-mediated knockdown or small-molecule inhibition, we tested the genotoxic
37 and cytotoxic effects of MTH1 deficiency on H23 (p53-mutated), H522 (p53-mutated) and A549
38 (wildtype p53) non-small cell lung cancer cell lines relative to normal MRC-5 lung fibroblasts. We also
39 assessed if MTH1 inhibition augments current therapies.

40 **Results:** MTH1 knockdown increased levels of oxidatively damaged DNA and DNA damage signaling
41 alterations in all lung cancer cell lines but not normal fibroblasts, despite no detectable differences
42 in reactive oxygen species levels between any cell lines. Furthermore, MTH1 knockdown reduced
43 H23 cell proliferation. However, unexpectedly, it did not induce apoptosis in any cell line or enhance
44 the effects of gemcitabine, cisplatin or radiation in combination treatments. Contrastingly, TH287
45 and TH588 MTH1 inhibitors induced apoptosis in H23 and H522 cells, but only increased oxidative
46 DNA damage levels in H23, indicating that they kill cells independently of DNA oxidation and
47 seemingly via MTH1-distinct mechanisms.

48 **Conclusions:** MTH1 has a NSCLC-specific p53-independent role for suppressing DNA oxidation and
49 genomic instability, though surprisingly the basis of this may not be reactive-oxygen-species-
50 associated oxidative stress. Despite this, overall our cell viability data indicates that targeting MTH1
51 will likely not be an across-the-board effective NSCLC therapeutic strategy; rather it induces non-
52 cytotoxic DNA damage that could promote cancer heterogeneity and evolution.

53 **Keywords**

54 Lung cancer, MTH1, NUDT1, targeted therapy, nucleotides, oxidative DNA damage, genomic
55 instability, combined therapy, gemcitabine, cisplatin

57 **Background**

58 Cancer cells harbour genetic mutations and exhibit phenotypic traits that are not found in normal
59 cells. These cancer-specific features may provide avenues for the development of targeted therapies
60 that selectively kill cancer cells [1]. The development of such strategies is a major focus of current
61 cancer research. One such approach is synthetic lethality, which is when an acquired defect in a
62 particular factor or pathway renders cancer cells sensitive to inhibition of another second specific
63 factor. Still, this approach is often limited to a certain context or cancer type, for example, inhibiting
64 poly(ADP-ribose) polymerase (PARP) in BRCA1- and BRCA2-deficient breast and ovarian cancers [2,
65 3]. An alternative though related strategy that may be more effective in treating a wider range of
66 cancers is cancer phenotypic lethality, which is to target factors and cell processes that are non-
67 essential in normal cells but that become essential for cell growth following the acquisition of
68 hallmark cancer traits [1, 4-6]. However, until such pathways are identified and validated for
69 therapeutic potential, radiotherapy- and chemotherapy-based treatments that are often associated
70 with side-effects and resistance will remain the mainstay of treatments.

72 Oxidative stress, which arises when there is an imbalance between the production of reactive
73 oxygen species (ROS) and the ability of a cell to counteract their levels or effects, is a hallmark cancer
74 trait that can drive both carcinogenesis and continuing tumour evolution [4, 7]. Paradoxically, ROS
75 are the basis of much of the cytotoxicity of radiotherapy and several chemotherapy treatments.
76 Hence, there may be several normally non-essential oxidative stress response factors and pathways
77 that become 'conditionally essential' in cancer cells and/or significantly affect therapy responses.

1
2
3
4
5
6
7
8
9
10
11
12
13
14
15
16
17
18
19
20
21
22
23
24
25
26
27
28
29
30
31
32
33
34
35
36
37
38
39
40
41
42
43
44
45
46
47
48
49
50
51
52
53
54
55
56
57
58
59
60
61
62
63
64
65

79 ROS can react with all components of DNA to cause numerous types of lesions [8]. However, the free
80 deoxyribonucleoside triphosphate (dNTP) pool is reportedly 190-13,000 times more susceptible to
81 modification than DNA [9]. This suggests that a significant proportion of oxidative-stress-induced
82 DNA damage arises via misincorporation of oxidised dNTPs during DNA replication rather than direct
83 DNA modification. Oxidised DNA bases do not majorly disrupt DNA structure; however, they can
84 subsequently lead to secondary types of DNA damage such as DNA mismatches [10], DNA single-strand
85 breaks (SSBs) that arise when DNA glycosylases remove damaged bases during base excision repair
86 (BER), and DNA double-strand breaks (DSBs) [11] that arise through poorly defined mechanisms
87 possibly due to DNA replication stress. DSBs in particular are highly genotoxic and cytotoxic if not
88 repaired correctly. This leads to the prediction that the pathways involved in preventing oxidised
89 DNA base misincorporation could be critical in either promoting or suppressing cancer development
90 and evolution depending on context [12].

91
92 Mut T Homologue 1 (MTH1) is a Nudix hydrolase family enzyme member that hydrolyses selected
93 oxidised dNTP and NTP substrates to the corresponding mono-phosphate products and inorganic
94 pyrophosphate to prevent their misincorporation into DNA and RNA respectively [13-15]. Primary
95 substrates of MTH1 are dNTPs containing 8-oxo-7,8-dihydroguanine (8-oxoGua), one of the most
96 common types of ROS-induced lesions [16], and 2-hydroxy-adenine. Supporting the idea of a role in
97 cancer cell maintenance, MTH1 levels are elevated in various cancers [17-21], while lower MTH1
98 levels in U2OS osteosarcoma cells and non-small cell lung cancer (NSCLC) patient samples correlates
99 with increased levels of DNA oxidation [22, 23]. MTH1 overexpression in oncogene-expressing
100 human cells promoted transformation [11, 24, 25], while knockdown lead to DNA-replication-
101 associated DNA damage response (DDR) activation and senescence [11, 26]. Accordingly, the first
102 developed MTH1 inhibitors appear to selectively inhibit cancer cell growth [22, 27]. Collectively,
103 these findings suggest that as cells undergo malignant transformation and acquire the trait of
104 oxidative stress, MTH1 becomes essential for maintaining genome integrity and cell viability. This

105 implies that targeting MTH1 activity could form the basis of a new targeted therapy strategy [1, 28].
106 However, other recent data challenged these observations and conclusions. In these studies, MTH1
107 deficiency did not hinder the growth of HeLa, SW480 or U2OS cells, and highly specific MTH1
108 inhibitors displayed only weak cancer cell cytotoxicity [29-31]. The title of the recent review, “MTH1
109 as a chemotherapeutic target: the elephant in the room” [32], highlights the fact that the differing
110 opinions and conclusions remain unresolved. Hence, it has become critically important to undertake
111 further work to shed light on these contradictory findings and better understand the relevance of
112 MTH1 in cancer and therapy.

113
114 Lung cancer is the leading cause of cancer death worldwide [33]. Despite improvements in survival
115 rates for many other cancer types in recent years, NSCLC therapy responses and patient outcomes
116 have not significantly improved [33, 34]. In our study, we addressed two main objectives to enable
117 the assessment of the potential of MTH1 inhibition as a NSCLC targeted therapy strategy. First, we
118 assessed if MTH1 deficiency alone is genotoxic or cytotoxic to several lung cell lines, and whether
119 these effects were highly selective to NSCLC cells relative to normal cells. Second, we evaluated
120 potential new combination therapy strategies by testing if targeting MTH1 enhanced the effects of
121 current therapeutic agents. Thus, we tackle the currently opposing and contentious opinions on the
122 significance of MTH1 in cancer biology and therapy [1, 35].

123

124 **Methods**

125 **Cell lines and chemicals**

126 A549 (CCL-185; wildtype p53), H522 (CRL-5810; p53 mutation c.572delC, p.P191fs*56), H23 (CRL-
127 5800; p53 mutation c.738G>C, p.M246I) and MRC-5 (CCL-171; wildtype p53) cell lines were
128 purchased fully authenticated from ATCC (p53 mutation information provided at
129 [https://www.atcc.org/Documents/Learning_Center/~media/5F7B1CCACF724E3398BE56BFBE3EFE](https://www.atcc.org/Documents/Learning_Center/~media/5F7B1CCACF724E3398BE56BFBE3EFE4.ashx)
130 4.ashx). MRC-5 and A549 cell lines were cultured in EMEM (ATCC) and DMEM-high glucose

131 (ThermoFisher Scientific) media respectively, and H522 and H23 cells in RPMI 1640 medium ATCC
132 modification. All media were supplemented with 10% (v/v) FBS (ThermoFisher Scientific). Cells were
133 cultured at 37°C in humidified atmosphere (95% air / 5% CO₂) and maintained at a low passage by
134 not passaging beyond 6 months' post resuscitation. Cisplatin, gemcitabine, VP-16 (etoposide),
135 phleomycin, hydroxyurea and MTH1 small molecule inhibitors (TH287, TH588) were purchased from
136 Sigma-Aldrich.

137

138 **siRNA transfections**

139 These were performed using DharmaFECT 1 reagent (GE Healthcare) according to manufacturer's
140 instructions. Briefly, a transfection complex was prepared by incubating together for 20 minutes at
141 room temperature, 7.5 µl DharmaFECT 1 reagent, 125 µl Opti-MEM medium (ThermoFisher
142 Scientific) and siRNA diluted in 125 µl Opti-MEM medium (final siRNA concentrations were 20 and 15
143 nM for H522 and remaining cell lines, respectively). 3 X 10⁵ cells were plated with the transfection
144 complex and incubated for 24 hours in Opti-MEM medium, after which the transfection media was
145 replaced with standard medium. MTH1-siRNA oligonucleotide 5'→3' sequences (ThermoFisher
146 Scientific) were sense CAUCUGGAAUUAACUGGAUtt and antisense AUCCAGUAAUCCAGAUGaa.
147 Silencer Select Negative Control 1 siRNA (ThermoFisher Scientific) was used as scramble siRNA
148 control.

149

150 **Modified alkaline comet assay**

151 DNA damage was assessed using Formamidopyrimidine-DNA glycosylase (Fpg)-modified comet assay
152 that is a slight modification of the original method [36]. Briefly, slides containing cells embedded in
153 0.6 % low melting point agarose were incubated overnight at 4°C in lysis buffer (2.5 M NaCl, 100 mM
154 Na₂EDTA, 10 mM Tris-base, 1 % Triton X-100, pH 10) (chemicals purchased from Sigma-Aldrich).
155 Lysed cells were treated with Fpg (final concentration 0.8 U/gel) for 30 minutes at 37°C, and
156 subjected to alkaline electrophoresis in buffer containing 300 mM NaOH, 1 mM Na₂EDTA, pH 13.

157 Following neutralization with 0.4 M Tris-base, pH 7.5, slides were stained with 2.5 µg/ml propidium
158 iodide (PI) and dried at 37°C. Comets were visualised at X200 magnification using an Olympus BH-2-
159 RFL-T2 fluorescent microscope fitted with an excitation filter of 515-535 nm and a 590 nm barrier
160 filter, and images were captured via a high performance CCD camera (COHU MOD 4912-
161 5000/0000). % tail DNA was calculated using Komet software (Andor Technology). For radiation
162 treatments, the Xstrahl RS320 X-Ray Irradiator system was used to expose agarose-embedded cells
163 on ice (assessments of immediate DNA damage) or cells in suspension that were then cultured for 24
164 hours (recovery samples). In the MTH1 inhibitor experiments, cells growing in complete medium
165 were treated with 10 µM TH287 or TH588 for 24 hours prior to collection.

166

167 **ROS level measurements**

168 30,000 cells per well were seeded in triplicate in black 96 well plates (Porvair) and cultured for 24
169 hours. Cells were washed with 200 µl PBS prior to the addition of 1 µl H2DCF-DA (ThermoFisher
170 Scientific) and incubated in the dark for 30 minutes in a humidified atmosphere at 37°C. 200 µl PBS
171 was then added to all the wells, and the relative ROS-induced fluorescence intensities were
172 measured immediately on a FLUOstar OPTIMA Microplate Reader (BMG Labtech; 485 nm excitation
173 and 520 nm emission wavelengths). 30-minute pre-treatment with 9.8 mM hydrogen peroxide was
174 used for positive controls (relatively high dose used to overcome the scavenging of extracellular
175 hydrogen peroxide by sodium pyruvate in the media [37]). Samples without seeded cells used as
176 blanks.

177

178 **WST-1 cell proliferation assay**

179 WST-1 is a water-soluble tetrazolium salt that is cleaved to a formazan dye in a mechanism mainly
180 dependent on NAD(P)H production by metabolically active cells. 2 days after transfection, 1 X 10⁴
181 cells (2 X 10⁴ for H522) were seeded in triplicate for each sample in clear flat bottom 96 well plates,
182 and left for 3 days before performing the assay according to manufacturer's instructions (Sigma-

183 Aldrich). Briefly, 10 μ l Cell Proliferation Reagent WST-1 was added to each well containing 100 μ l
184 media and incubated for between 30 minutes to 4 hours. Absorbance values (that ranged between
185 0.5-2) were determined on an ELx808 microplate reader (BIO-TEK Instruments) at 450 nm against a
186 blank control background. Cell proliferation (%) was determined by calculating (mean absorbance of
187 sample / mean absorbance of control) X 100. 2-day VP-16 (Sigma-Aldrich) treatments were used as
188 positive controls.

189

190 **Annexin V/PI apoptosis assay**

191 Double staining with annexin V-FITC (apoptosis marker)/PI combined with flow cytometry was
192 applied as described in manufacturer's instructions (Affymetrix). VP-16 was used as a positive
193 control, while 4 untreated negative control cells were included for instrumental compensation and
194 gating: no stain, PI only, annexin V-FITC only, and both PI and annexin V-FITC. Samples were
195 analysed on a BD FACSCanto™ II flow cytometer (BD Biosciences) using BD FACSDiVa™ v6.1.3
196 software. At least 10,000 events were acquired per sample.

197

198 **Western blot analysis**

199 Standard techniques were used. Briefly, protein samples were prepared using Laemmli buffer lysis
200 and sonication (15 seconds at 14 μ m using Soniprep 150). MTH1, MTH2 and α -tubulin antibodies
201 were purchased from Abcam, and CHK1 (2G1D5), phospho-CHK1 (Ser345), phospho-CHK2 (Thr68)
202 from Cell Signaling Technology. Polyclonal secondary antibodies were horseradish-peroxidase-
203 conjugated, and detection was performed using ECL substrate (Pierce) and X-ray film (CL-XPosure).
204 Band intensities were quantified using densitometry GeneSnap or Image J 1.49 version software.

205

206 **Data analysis and statistical tests.** GraphPad Prism software (version 7 and 6.05) was used to
207 calculate mean \pm standard deviation (S.D) or standard error mean (SEM). Unless otherwise stated in
208 the figure legend, data was evaluated by one-way ANOVA followed by post-hoc Tukey's multiple

209 comparison test to compare values between two or more groups. P-value < 0.05 was considered as
210 statistically significant. The number of independent experimental repeats are indicated in each
211 figure or figure legend.

212

213 **Results**

214 **MTH1 deficiency increases levels of DNA oxidation in NSCLC cells but not normal lung fibroblasts**

215 In order to observe the effects of MTH1 deficiency we used siRNA to successfully knockdown MTH1
216 in various lung cell lines. We targeted MTH1 in H23 adenocarcinoma (p53-mutated), H522
217 adenocarcinoma (p53-mutated) and A549 lung carcinoma (wildtype p53) NSCLC cell lines in order to
218 assess if any observed effects are applicable to NSCLC in general and/or are dependent on p53
219 status, and in MRC-5 normal lung cells to determine if the effects are cancer specific. Though MTH1
220 is elevated in some cancers [17-21], endogenous MTH1 levels were not significantly different
221 between the NSCLC and MRC-5 cell lines. H522 had the lowest MTH1 level, but the levels in H23,
222 A549 and MRC-5 were only 1.3-, 1.4- and 1.2-fold higher, respectively (Additional File 1). MTH1
223 levels were significantly reduced 3 days after MTH1 siRNA transfection, averaging decreases of 88%
224 in H23, 83% in A549 and 76% in MRC-5, and remained low for at least 6 days (Fig. 1A, 1B and 1D).
225 MTH1 knockdown efficiency was slightly delayed in H522 cells, but MTH1 levels still decreased by
226 70% inhibition by day 4 (Fig. 1C). The levels of MTH1 depletion were comparable to those in previous
227 published studies [11, 38]. Hence, using siRNA we were able to study the role of MTH1 in various
228 NSCLC cell lines and normal lung cells. The level of another Nudix hydrolase family enzyme member,
229 MTH2, did not increase following MTH1 knockdown (Additional file 2), suggesting it does not act to
230 compensate for loss of MTH1. This is concordant with a recent study that found MTH2 has a
231 preference for nucleotide substrates different to those of MTH1 [39].

232

233 To begin to determine if significantly reduced MTH1 levels lead to functional consequences in
234 different lung cell lines, we first assessed the effects of MTH1 knockdown on DNA oxidation levels

1 235 using the Fpg-modified alkaline comet assay (Additional file 3). Cells were collected 4 days after
2 236 siRNA transfection to provide sufficient time for them to have undergone DNA replication in the
3
4 237 presence of notably reduced MTH1 levels. Following MTH1 knockdown, we consistently observed
5
6 238 significant 1.5- to 2-fold increases in oxidatively damaged DNA bases (i.e. Fpg-sensitive sites) in H23,
7
8
9 239 H522 and A549 genomic DNA relative to the scrambled siRNA controls, but no difference in MRC-5
10
11 240 (Fig. 2A to 2D). This finding is concordant with the notion that MTH1 acts to suppress the
12
13 241 misincorporation of oxidised dNTPs specifically in cancer cells. We observed no increases in DNA SSB
14
15 242 levels (i.e. Fpg-independent sites), which contrasts with a previous observation in A549 cells [25].
16
17 243 The reason for this contradiction is unclear; however, unless a cell line also harbours a BER defect
18
19 244 that leads to the generation of more or longer-lived SSB intermediates following initial damaged
20
21 245 base removal [40], we would not predict an increase in SSB levels following MTH1 knockdown.
22
23
24
25

26 246

27
28 247 To assess if the conditional requirement for MTH1 is due to cancer-associated oxidative stress we
29
30 248 measured ROS levels in all cell lines. However, we found no differences between any of the NSCLC
31
32 249 lines and MRC-5 (Fig. 2E). This is consistent with there being no significant differences between any
33
34 250 of the cell lines in the background levels of DNA oxidation and SSBs (Fig. 2A to 2D), but implies that
35
36 251 the basis of the requirement for MTH1 to suppress DNA oxidation in NSCLC cells is not simply due to
37
38 252 higher ROS levels. This finding goes against previous proposed models [22, 25]. Given all the genetic
39
40 253 and signaling disturbances within cancer cells, there may be many other causes of this MTH1
41
42 254 dependency that remain to be discovered.
43
44
45
46

47 255

48 256 **MTH1 is not required in response to exogenous sources of oxidative stress**

49
50 257 Hydrogen peroxide treatment was previously shown to lead to the accumulation of genomic 8-
51
52 258 oxoGua and cell death in *MTH1*^{-/-} mouse embryonic fibroblasts [41], indicating that oxidative stress
53
54 259 can be cytotoxic in a MTH1-deficient background. We proposed that in addition to a role in
55
56 260 processing endogenously-generated oxidised dNTPs within NSCLC cells, MTH1 would also be
57
58
59
60
61
62
63
64
65

1
2
3
4
5
6
7
8
9
10
11
12
13
14
15
16
17
18
19
20
21
22
23
24
25
26
27
28
29
30
31
32
33
34
35
36
37
38
39
40
41
42
43
44
45
46
47
48
49
50
51
52
53
54
55
56
57
58
59
60
61
62
63
64
65

261 required to suppress the misincorporation of damaged DNA bases following exposure to exogenous
262 sources of oxidative stress and anti-cancer agents. To determine this, we first assessed whether
263 higher DNA oxidation levels were detectable in MTH1-deficient H23 cells after irradiation (IR)
264 treatment, which targets the nucleotide pool [42]. Cell samples were analysed immediately after IR
265 and following a 24-hour recovery, which was permitted to allow enough time for IR-generated
266 oxidised dNTPs to be misincorporated. The relative increases in SSB levels and oxidatively damaged
267 DNA immediately after IR did not differ between the scramble siRNA control and MTH1-deficient
268 cultures (Fig. 2F), confirming that MTH1 does not have a role in preventing direct oxidation of DNA.
269 However, by 24 hours post-IR, the relative levels of oxidatively damaged DNA in all samples had
270 returned to levels comparable to those prior to IR. A similar observation was seen when oxidative
271 stress was induced after treatment with the model oxidant (non-radical ROS), hydrogen peroxide
272 (Additional file 4). Overall, this suggests that MTH1 is not required to prevent the misincorporation
273 of dNTPs that are oxidised via exogenous agents. Alternatively, other MTH1-independent
274 compensatory factors such as Ogg1 may be activated when very high levels of damaged dNTPs are
275 acutely generated [43].

276

277 **MTH1 deficiency induces alterations in DNA damage response signaling**

278 We propositioned that the increased levels of oxidised DNA bases caused by MTH1 knockdown may
279 lead to DNA replication stress in NSCLC cell lines, while normal cells would remain genomically
280 stable. The central kinase pathways in the DNA-replication-associated DDR are ATR-CHK1 and ATM-
281 CHK2, which are initially activated by defective DNA replication forks and DSBs respectively [44].
282 Using Western blotting, we detected indications of DDR alterations in all NSCLC cells lines following
283 MTH1 knockdown (Fig. 3), suggesting that the cells were responding to replication stress and some
284 kind of secondary DNA damage. Surprisingly, however, the DDR responses in different NSCLC cell
285 lines varied in the pathways affected and whether they were activated or repressed.

286

1
2
3
4
5
6
7
8
9
10
11
12
13
14
15
16
17
18
19
20
21
22
23
24
25
26
27
28
29
30
31
32
33
34
35
36
37
38
39
40
41
42
43
44
45
46
47
48
49
50
51
52
53
54
55
56
57
58
59
60
61
62
63
64
65

287 We detected DDR activation in MTH1-knockdown H522 cells, as indicated by an approximately 2-fold
288 increase in CHK2 phosphorylation levels relative to no siRNA and scramble siRNA controls (Fig. 3A
289 and 3B). This is indicative of the presence of DSBs, as shown by use of the topoisomerase II inhibitor
290 VP-16 as a positive control. In contrast, we repeatedly detected notable losses of CHK1 protein levels
291 in MTH1-knockdown H23 and A549 cells relative to no siRNA and scramble siRNA controls, which
292 was significant in A549 relative to no siRNA, but no indications of increased CHK1 phosphorylation in
293 any cell line (Fig. 3C and 3D). The basis of the CHK1 down-regulation is not clear. It may indicate that
294 MTH1-deficient H23 and A549 cells had increased DNA replication stress levels, but that there was a
295 selective pressure to rapidly adapt and down-regulate associated ATR-CHK1 activity to overcome
296 growth arrest. Transfection with the scrambled siRNA caused increased Chk1 levels in H23 and H522
297 cells. The reason for this is unclear, but it is very likely due to unavoidable transfection-dependent
298 siRNA-independent effects on these particular cell lines as the commercially available scrambled
299 siRNA used (Silencer Select Negative Control No. 1, ThermoFisher Scientific) has no significant
300 sequence similarity to human gene sequences and is confirmed to have minimal effects on gene
301 expression. Nonetheless, the fact that lower Chk1 levels were detected in H23 and A549 MTH1
302 siRNA cultures even relative to the basal no siRNA (no transfection) cultures demonstrates the
303 strength of the phenotype. Finally, in our experimental conditions we could not detect total CHK1 in
304 MRC-5 cells (ATCC CCL-171), as indicated by a previous study [45]. This may be due to very low
305 relative expression levels and/or an issue with the particular antibody used.

306 307 **MTH1 promotes H23 cell proliferation, but is dispensable for NSCLC cell survival**

308 Given the observed function for MTH1 in genome maintenance, we hypothesised that MTH1 would
309 be 'conditionally essential' in NSCLC cells. To first test this, we assessed if MTH1 was required for
310 NSCLC cell proliferation using the WST-1 assay, which measures the metabolic activity in cell
311 cultures. Concordant with the indication in Fig. 3 that H23 and H522 cell lines are slightly sensitive to
312 the non-specific effects of transfection, the scrambled siRNA transfected cultures showed 20 % and

313 30 % decreases in cell proliferation, respectively (Fig. 4A and 4C). Nevertheless, MTH1 knockdown
314 induced a significant 54 % and 34 % decrease in H23 cell proliferation relative to the no siRNA and
315 scrambled siRNA controls, respectively (Fig. 4A), indicating that MTH1 is partially required for H23
316 growth. However, similar decreases in cell proliferation were not seen in A549, H522 or MRC-5 cells
317 relative to controls (Fig. 4B to 4D). This contradicts previous data that suggested MTH1-deficient
318 A549 cells have dramatic proliferation defects [25].

319
320 To determine if MTH1 deficiency in NSCLC induces cell death in addition to or rather than cell growth
321 inhibition, we measured apoptosis levels using annexin V (Fig. 5A). We did not observe increased
322 apoptosis levels in any MTH1 knockdown cell cultures relative to the scrambled siRNA controls
323 irrespective of the p53-status of the line (Fig. 5B to 5E). Consistent with previous observations (Fig. 3
324 and 4), H23 and H522 scrambled siRNA cultures demonstrated minor MTH1-independent
325 transfection-dependent effects. The results of the apoptosis assay were confirmed using another
326 MTH1 siRNA that induces a similar decrease in MTH1 levels (Additional file 5).

327
328 Though MTH1 inhibition alone did not cause apoptosis, we propositioned that it would still enhance
329 the targetting and effectiveness of current chemotherapy agents that induce oxidative stress [46, 47]
330 and DNA replication stress. The basis of this idea was that MTH1 inhibition leads to higher levels of
331 oxidatively damaged DNA in NSCLC cells but not normal cells, which when combined with therapy-
332 induced effects selectively pushes the DNA damage levels over the cytotoxic threshold in NSCLC
333 cells. In particular, the mechanisms of action of gemcitabine and cisplatin suggests the combining
334 them with the effects of MTH1 inhibition could lead to additive or synergistic effects that would
335 improve patient outcomes. Gemcitabine is a chemical antimetabolite and analogue of deoxycytidine
336 that induces DNA replication stress [48-50], and cisplatin leads to DNA replication defects via the
337 formation of DNA crosslinks [51, 52] and can increase intracellular ROS levels possibly through
338 mitochondrial dysfunction and activation of NAD(P)H oxidase and superoxide production [53-55].

339

1
2 340 We treated H23 and H522 MTH1 knockdown cells with gemcitabine or cisplatin and monitored
3
4 341 apoptosis levels. The effect on H522 was of particular interest, as relative to H23 and A549, this cell
5
6 342 line displays much higher resistance to etoposide, gemcitabine and hydrogen peroxide (Fig. 5 and
7
8
9 343 Additional file 6). Despite our predictions, a combination of MTH1 knockdown with either
10
11 344 gemcitabine or cisplatin treatment did not lead to significant increases in cell death levels relative to
12
13 345 the treated scramble siRNA controls (Fig. 5F and 5G). These results were reproducible with a
14
15 346 different MTH1 siRNA (Additional file 5). This demonstrates that the oxidative DNA damage induced
16
17
18 347 by MTH1 deficiency in NSCLC cells does not sufficiently sensitise them to the effects of current
19
20
21 348 therapeutic agents.

22
23 349

24 25 350 **TH287 and TH588 MTH1 inhibitors have variable effects on NSCLC cell lines**

26
27
28 351 Using siRNA to assess the effects of MTH1 deficiency on lung cell lines had uncovered some
29
30 352 observations that agreed with our predictions, but also uncovered some unexpected results. To
31
32 353 confirm our findings, we similarly used the small molecule MTH1 inhibitors, TH287 and TH588, which
33
34
35 354 were previously shown to lead to a dramatic increase in oxidatively damaged DNA and loss of
36
37
38 355 viability in cancer cells but not primary human fibroblasts [22, 38].

39
40 356

41
42 357 When NSCLC and MRC-5 cell lines were treated with the same dose (10 μ M) of TH287 and TH588, an
43
44 358 observable though not significant increase in the levels of oxidatively damaged DNA was evident
45
46
47 359 only in H23 cells (Fig. 6A to 6D), implying that TH287 and TH588 treatments did not lead to increased
48
49
50 360 oxidatively damaged DNA in H522, A549 or MRC-5 cells. There was no increase in SSB levels in any
51
52 361 cell line following TH287 or TH588 treatment (Fig. 6A to D), which contrasts with a previous
53
54 362 observation in U2OS osteosarcoma cells [22]. We next assessed if the levels of oxidatively damaged
55
56
57 363 DNA correlated apoptosis induction. Indeed, TH287 and TH588 induced significant 3.2 and 3.0-fold
58
59 364 increases in apoptosis levels in H23 cells, respectively (Fig. 6E), and did not affect A549 cells (Fig. 6F).

1
2
3
4
5
6
7
8
9
10
11
12
13
14
15
16
17
18
19
20
21
22
23
24
25
26
27
28
29
30
31
32
33
34
35
36
37
38
39
40
41
42
43
44
45
46
47
48
49
50
51
52
53
54
55
56
57
58
59
60
61
62
63
64
65

365 However, significant 2.8 and 3.5-fold increases in apoptosis levels were also observed in inhibitor-
366 treated H522 cells (Fig. 6G), indicating that levels of DNA oxidation were not the major basis of the
367 cytotoxic effects. Normal MRC-5 lung fibroblasts did not exhibit any apoptotic response to TH287
368 and TH588 (Fig. 6H), agreeing with the original suggestion that TH287 and TH588 are not cytotoxic to
369 normal cells [22]. Collectively, these data suggest that TH287 and TH588 at the dose used induce cell
370 death in p53-mutated cancer cells through 'off target effects' rather than inhibition of MTH1, and do
371 not induce cell death in p53-proficient NSCLC cells and normal cells.

372

373 **Discussion**

374 In this study we tested the potential of a new targeted therapy strategy for NSCLC, whilst
375 simultaneously analysing opposing opinions within the field regarding the conditionally essential
376 requirements for MTH1 in cancer cells and whether the current pursuit of MTH1 inhibitor
377 development is likely to yield effective therapeutic agents [1, 32, 35]. We show that MTH1 does
378 indeed have a NSCLC-specific role for maintaining genome stability. The basis of this cancer-
379 specificity remains unclear, as DNA oxidation levels in MTH1-deficient lung cells do not correlate
380 with background ROS levels. This goes against the current model [32], and suggests that perhaps the
381 NSCLC-specific effect could be due to downstream defects in removing the oxidatively damaged DNA
382 induced in the cancer cell lines [56, 57]. Despite the functional role for MTH1 in NSCLC cells, we
383 show that MTH1 deficiency ultimately does not cause NSCLC death, either alone or when combined
384 with other therapeutic agents. One possibility for this could have been that the cell culture media
385 used contained sodium pyruvate, a ROS scavenger. However, we do not believe this to be the case
386 as sodium pyruvate scavenges extracellular ROS rather than intracellular endogenous ROS [37, 58],
387 and from what we can tell, other MTH1 studies that reported cytotoxic effects associated with MTH1
388 also used media containing sodium pyruvate [11, 22, 29]. Ultimately, our work argues that MTH1
389 inhibitors will likely not be effective therapeutic agents. Instead, given that we show that MTH1
390 deficiency in NSCLC cells induces non-cytotoxic DNA oxidation and DDR alterations, we propose that

1 391 treating NSCLC patients with MTH1 inhibitors could actually provide an environment for further
2 392 mutation accumulation to drive cancer heterogeneity and evolution. In accordance with this
3
4 393 proposition, MTH1-knockdown in human B lymphoblastoid cells induces a higher mutation rate but
5
6 394 not cell death after UVA-induced oxidative stress [59], while MTH1 overexpression repressed the
7
8
9 395 DNA-replication-dependent mutator phenotype in mismatch-repair-defective colorectal cancer cells
10
11 396 [60].
12

13 397
14
15
16 398 The increases in oxidatively damaged DNA in NSCLC cell lines following MTH1 knockdown was
17
18 399 relatively small (Fig. 2). However, the alterations in DDR signaling indicate that this was enough to
19
20
21 400 disrupt DNA replication and lead to secondary types of DNA damage such as DSBs (Fig. 3). One
22
23 401 proposed model for how this occur is that oxidised DNA bases induce DNA replication stress, which
24
25 402 is defined as defective DNA replication fork progression [61, 62], and that this somehow
26
27 403 subsequently leads to DSBs [22, 27]. It is possible that DSBs can arise from replication fork run-off at
28
29 404 BER-induced SSBs, which would lead to the generation of one-ended broken DNA replication forks in
30
31 405 a mechanism analogous to DSBs arising from Top1-DNA adducts [63]. Alternatively, DNA replication
32
33 406 forks may stall at sites of oxidatively damaged DNA and be cleaved by endonucleases such as Mus81
34
35 407 to also generate one-ended broken replication forks [64, 65]. No matter how they arise, these one-
36
37 408 ended DNA DSBs on replicating chromosomes would lead to Chk2 activation [65], and are potentially
38
39 409 highly genotoxic or cytotoxic as they may be very difficult to resolve. Concordantly, one-ended DNA
40
41 410 DSBs are linked to various types of mutations [66-69].
42

43 411
44
45
46
47 412 It is unclear why the DDR signaling alterations varied between the MTH1-defective NSCLC lines (Fig.
48
49 413 3), but given that different cancers already harbour many other mutations and potentially DDR
50
51 414 defects, the signaling variances may simply reflect the differing abilities and deficiencies in DDR
52
53 415 functions in different cancers. Furthermore, ultimately the ATM/CHK2 and ATR/CHK1 pathways are
54
55 416 interlinked, as ATM-activating DSBs can subsequently lead to ATR activation if they are resected to
56
57
58
59
60
61
62
63
64
65

1
2
3
4
5
6
7
8
9
10
11
12
13
14
15
16
17
18
19
20
21
22
23
24
25
26
27
28
29
30
31
32
33
34
35
36
37
38
39
40
41
42
43
44
45
46
47
48
49
50
51
52
53
54
55
56
57
58
59
60
61
62
63
64
65

417 generate ssDNA overhangs [70], and processing of ATR-activating stalled forks can generate DSBs
418 [64]. The induction of phosphorylated CHK2 in H522 cells suggests that DNA DSBs arise. Why this
419 should only occur or be detectable in H522 cells remains unclear. The reasons for decreased total
420 CHK1 levels in A549 and H23 cell cultures were surprising. Although DDR activation following MTH1
421 knockdown was previously observed, including phosphorylation of H2AX, 53BP1, ATM and DNA-PKcs
422 [11, 22, 24, 27], to our knowledge this is the first time that a MTH1-knockdown-associated 'switching
423 off' of the DDR has been observed. Induced deficiency of a DDR factor may indicate that MTH1
424 knockdown in A549 and H23 cells initially induces DNA replication fork stalling and ATR/CHK1
425 activation, but that the bulk of the cells efficiently turned off this cell cycle checkpoint signaling by
426 lowering CHK1 levels to continue proliferating. Given that CHK1 levels were decreased within 4 days
427 of MTH1 knockdown, this would not be enough for a mutation and clonal expansion to occur within
428 the population, suggesting CHK1 suppression occurs through another mechanism that may involve
429 changes in gene expression (epigenetic), RNA processing, post-translational modifications and/or
430 proteosomal degradation. Accordingly, various stresses have previously been linked to CHK1
431 degradation [71, 72].

432
433 There have been several contradictory and opposing reports on the cytotoxicity of MTH1 deficiency
434 using various siRNA and shRNA sequences, cell lines and inhibitors [11, 22, 24, 26, 27, 29-31, 38],
435 which were recently summarized and compared in a review article [32]. A critical finding of our work
436 is, that despite MTH1 deficiency causing genomic instability in NSCLC cells and decreased H23 cell
437 proliferation, there was a lack of cytotoxicity associated with MTH1 knockdown in all NSCLC cell lines
438 (Fig. 5). A simple explanation for this finding is that the levels of MTH1 knockdown in our
439 experiments were not sufficient enough to induce MTH1 deficiency. Or, as already discussed, other
440 factors may be able to sufficiently compensate for MTH1 [43]. However, we do not believe either of
441 these possibilities is the basis of the disparities, as the 1.5- to 2-fold increase in oxidatively damaged
442 DNA damage (Fig. 2) is comparable to that in other studies that did detect loss of cancer cell viability

1
2
3
4
5
6
7
8
9
10
11
12
13
14
15
16
17
18
19
20
21
22
23
24
25
26
27
28
29
30
31
32
33
34
35
36
37
38
39
40
41
42
43
44
45
46
47
48
49
50
51
52
53
54
55
56
57
58
59
60
61
62
63
64
65

443 [11, 22, 26, 38]. Also, we performed our experiments 4 days after transfection, which was before
444 MTH1-proficient cells could take over culture (as confirmed by Western blot, Fig. 1). Hence, we
445 suggest that the increased levels of genomic instability in MTH1-deficient NSCLC cells is not
446 sufficiently high enough to induce cell death, rather it could promote further mutations and
447 heterogeneity. Overall, our data therefore indicates that MTH1 inhibition will likely not be a
448 successful therapeutic strategy for many NSCLC patients even when used in combination
449 treatments. However, it remains possible that the effects of MTH1 deficiency vary considerably
450 depending on circumstances. For example, MTH1 inhibition may be more effective on cancer cells
451 that exhibit very high oxidative stress or particular possess mutations, and combining MTH1
452 inhibition with other specific agents or inhibitors (for example, Chk2 inhibitors) may prove to be
453 selectively toxic.

454
455 The MTH1 small molecule inhibitors, TH287 or TH588, were proposed to be effective for cancer cell
456 killing due to MTH1 inhibition [22]. In our studies, TH287 and TH588 did induce apoptosis in 2 out of
457 the 3 NSCLC cell lines tested, but this did not entirely correlate with increases in oxidatively damaged
458 DNA levels (Fig. 6). This suggests that the effects on cell viability may have been distinct from MTH1
459 inhibition. Accordingly, the cytotoxicity of TH588 to melanoma cells was recently suggested to
460 correlate to endogenous ROS levels but be independent of MTH1, as TH588 treatment induced
461 melanoma cell death but MTH1 knockdown did not, and TH588-induced apoptosis is not rescued by
462 overexpressing MTH1 or introducing the bacterial homolog of MTH1 that is not inhibited by TH588
463 [73]. It was also recently proposed that TH287 or TH588 at the dose we used exert much of their
464 cytotoxic effects through tubulin polymerisation defects [30], though this conclusion was
465 subsequently challenged as TH588 does not induce cellular changes commonly associated with
466 Paclitaxel-induced tubulin defects [38]. Repeating the TH287 and TH588 treatments at a lower dose
467 of 3 μ M, which does not induce tubulin polymerisation defects [30], and over a longer time period
468 may more specifically assess the consequences of TH287/TH588-induced MTH1 inhibition on NSCLC

1
2 469 cells. Nonetheless, other highly specific MTH1 inhibitors were found to not be cytotoxic to cancer
3 470 cells [29, 31]. This not only supports the conclusion that MTH1 is not essential for NSCLC cell
4 471 viability, but also strengthens the argument that MTH1 inhibitors may not make effective
5 472 therapeutic agents.
6
7
8

9 473

10 11 474 **Conclusion**

12
13
14 475 The importance of the MTH1 enzyme in cancer is a highly controversial topic within current cancer
15
16 476 research and the focus of intense study. We show that MTH1 is indeed selectively required in
17
18 477 various NSCLC cell lines to maintain genome integrity and support H23 cell proliferation. However,
19
20 478 unexpectedly, MTH1 is ultimately not essential for NSCLC cell viability and does not alter responses
21
22 479 to current therapeutic agents. Thus, our work indicates that MTH1 is likely not an effective
23
24 480 therapeutic target for NSCLC. On the contrary, inhibiting MTH1 may promote further mutation
25
26 481 accumulation and disease progression.
27
28
29

30 482

31 32 33 483 **List of abbreviations**

34
35 484 BER: base excision repair; DSB: DNA double-strand breaks; DDR: DNA damage response; dNTP:
36
37 485 deoxyribonucleoside triphosphate; Fpg: Formamidopyrimidine-DNA glycosylase; PARP: poly(ADP-
38
39 486 ribose) polymerase; MTH1: Mut T Homologue 1; NSCLC: non-small cell lung cancer; PI: propidium
40
41 487 iodide; ROS: reactive oxygen species; 8-oxoGua: 8-oxo-7,8-dihydroguanine; SSB: single-strand break.
42
43
44

45 488

46 47 489 **Ethics approval and consent to participate**

48
49 490 Not applicable
50
51

52 491

53 54 492 **Consent for publication**

55
56 493 Not applicable
57
58
59 494

495 **Availability of data and materials**

1
2 496 The datasets used and/or analysed during the current study are available from the corresponding
3
4 497 author upon reasonable request.
5
6

7 498

8
9 499 **Competing interests**

10
11 500 The authors declare that they have no competing interests
12
13

14 501

15
16 502 **Funding**

17
18 503 HHKA was funded by the Iraqi Cultural Attache (UK) under a PhD studentship award.
19
20

21 504

22
23 505 **Author contributions**

24
25 506 SSF, GDDJ and MDE conceived and designed the experiments. HHKA performed the experiments.
26
27

28 507 KMHA significantly contributed to the conception and design of the WST-1 assay experiments and to
29
30

31 508 the interpretation of the data. HHKA, SSF, GDDJ and MDE analyzed the data. SSF, GDDJ, MDE and
32
33

34 509 HHKA wrote the paper. All authors read and approved the final manuscript.
35
36

37 510

38 511 **Acknowledgements**

39
40 512 We thank the Leicester Imaging Technologies facility (LITE) within the Centre for Core Biotechnology
41
42

43 513 Services of the University of Leicester for use of the flow cytometers. We also thank Kamla Alsalmani
44
45

46 514 for providing training to HHKA.
47
48

49 515

50 516 **References**

51
52
53 517 1. Helleday T. Cancer phenotypic lethality, exemplified by the non-essential MTH1 enzyme being
54
55

56 518 required for cancer survival. Ann Oncol. 2014;25(7):1253.
57
58
59
60
61
62
63
64
65

- 1
2
3
4
5
6
7
8
9
10
11
12
13
14
15
16
17
18
19
20
21
22
23
24
25
26
27
28
29
30
31
32
33
34
35
36
37
38
39
40
41
42
43
44
45
46
47
48
49
50
51
52
53
54
55
56
57
58
59
60
61
62
63
64
65
- 519 2. Bryant HE, Schultz N, Thomas HD, Parker KM, Flower D, Lopez E, et al. Specific killing of BRCA2-
520 deficient tumours with inhibitors of poly(ADP-ribose) polymerase. *Nature*. 2005;434(7035):913-917.
 - 521 3. Farmer H, McCabe N, Lord CJ, Tutt AN, Johnson DA, Richardson TB, et al. Targeting the DNA repair
522 defect in BRCA mutant cells as a therapeutic strategy. *Nature*. 2005;434(7035):917-921.
 - 523 4. Liou G, Storz P. Reactive oxygen species in cancer. *Free Radic Res*. 2010;44(5):479-496.
 - 524 5. Toledo LI, Murga M, Fernandez-Capetillo O. Targeting ATR and Chk1 kinases for cancer treatment:
525 A new model for new (and old) drugs. *Mol Oncol*. 2011;5(4):368-373.
 - 526 6. Puigvert JC, Sanjiv K, Helleday T. Targeting DNA repair, DNA metabolism and replication stress as
527 anti-cancer strategies. *FEBS J*. 2016;283(2):232-245.
 - 528 7. Kumar B, Koul S, Khandrika L, Meacham RB, Koul HK. Oxidative stress is inherent in prostate
529 cancer cells and is required for aggressive phenotype. *Cancer Res*. 2008;68(6):1777-1785.
 - 530 8. Dizdaroglu M, Jaruga P. Mechanisms of free radical-induced damage to DNA. *Free Radic Res*.
531 2012;46(4):382-419.
 - 532 9. Topal MD, Baker MS. DNA Precursor Pool: A significant target for N-methyl-N-nitrosourea in
533 C3H/10T1/2 clone 8 cells. *Proc Natl Acad Sci U.S.A*. 1982;79(7):2211-2215.
 - 534 10. Shibutani S, Takeshita M, Grollman AP. Insertion of specific bases during DNA synthesis past the
535 oxidation-damaged base 8-oxodG. *Nature*. 1991;349(6308):431-434.
 - 536 11. Rai P, Onder TT, Young JJ, McFaline JL, Pang B, Dedon PC, et al. Continuous elimination of
537 oxidized nucleotides is necessary to prevent rapid onset of cellular senescence. *Proc Natl Acad Sci*
538 *U.S.A*. 2009;106(1):169-174.
 - 539 12. Olinski R, Gackowski D, Rozalski R, Foksinski M, Bialkowski K. Oxidative DNA damage in cancer
540 patients: a cause or a consequence of the disease development? *Mutat Res Fund Mol Mech Mut*.
541 2003;531(1):177-190.
 - 542 13. Sakumi K, Furuichi M, Tsuzuki T, Kakuma T, Kawabata S, Maki H, et al. Cloning and expression of
543 cDNA for a human enzyme that hydrolyzes 8-oxo-dGTP, a mutagenic substrate for DNA synthesis. *J*
544 *Biol Chem*. 1993;268(31):23524-23530.

- 1
2
3
4
5
6
7
8
9
10
11
12
13
14
15
16
17
18
19
20
21
22
23
24
25
26
27
28
29
30
31
32
33
34
35
36
37
38
39
40
41
42
43
44
45
46
47
48
49
50
51
52
53
54
55
56
57
58
59
60
61
62
63
64
65
- 545 14. Fujikawa K, Kamiya H, Yakushiji H, Nakabeppu Y, Kasai H. Human MTH1 protein hydrolyzes the
546 oxidized ribonucleotide, 2-hydroxy-ATP. *Nucleic Acids Res.* 2001;29(2):449-454.
- 547 15. Nissink JWM, Bista M, Breed J, Carter N, Embrey K, Read J, et al. MTH1 substrate recognition—an
548 example of specific promiscuity. *PloS One.* 2016;11(3):e0151154.
- 549 16. van Loon B, Markkanen E, Hübscher U. Oxygen as a friend and enemy: How to combat the
550 mutational potential of 8-oxo-guanine. *DNA Repair.* 2010;9(6):604-616.
- 551 17. Kennedy CH, Cueto R, Belinsky SA, Lechner JF, Pryor WA. Overexpression of hMTH1 mRNA: a
552 molecular marker of oxidative stress in lung cancer cells. *FEBS Letters.* 1998;429(1):17-20.
- 553 18. Kennedy CH, Pass HI, Mitchell JB. Expression of human MutT homologue (hMTH1) protein in
554 primary non-small-cell lung carcinomas and histologically normal surrounding tissue. *Free Radic Biol*
555 *Med.* 2003;34(11):1447-1457.
- 556 19. Okamoto K, Toyokuni S, Kim WJ, Ogawa O, Takechi Y, Arai S, et al. Overexpression of human
557 mutT homologue gene messenger RNA in renal-cell carcinoma: evidence of persistent oxidative
558 stress in cancer. *Int J Cancer.* 1996;65(4):437.
- 559 20. Wani G, Milo GE, D'Ambrosio SM. Enhanced expression of the 8-oxo-7,8-dihydrodeoxyguanosine
560 triphosphatase gene in human breast tumor cells. *Cancer Lett.* 1998;125(1-2):123-130.
- 561 21. Tu Y, Wang Z, Wang X, Yang H, Zhang P, Johnson M, et al. Birth of MTH1 as a therapeutic target
562 for glioblastoma: MTH1 is indispensable for gliomatumorigenesis. *Am J Transl Res.* 2016;8(6):2803-
563 2811.
- 564 22. Gad H, Koolmeister T, Jemth AS, Eshtad S, Jacques SA, Strom CE, et al. MTH1 inhibition eradicates
565 cancer by preventing sanitation of the dNTP pool. *Nature.* 2014;508(7495):215-221.
- 566 23. Speina E, Arczewska KD, Gackowski D, Zielinska M, Siomek A, Kowalewski J, et al. Contribution of
567 hMTH1 to the maintenance of 8-oxoguanine levels in lung DNA of non-small-cell lung cancer
568 patients. *J Natl Cancer Inst.* 2005;97(5):384-395.

- 1
2
3
4
5
6
7
8
9
10
11
12
13
14
15
16
17
18
19
20
21
22
23
24
25
26
27
28
29
30
31
32
33
34
35
36
37
38
39
40
41
42
43
44
45
46
47
48
49
50
51
52
53
54
55
56
57
58
59
60
61
62
63
64
65
- 569 24. Rai P, Young JJ, Burton DGA, Giribaldi MG, Onder TT, Weinberg RA. Enhanced elimination of
570 oxidized guanine nucleotides inhibits oncogenic RAS-induced DNA damage and premature
571 senescence. *Oncogene*. 2011;30(12):1489-1496.
- 572 25. Patel A, Burton DGA, Halvorsen K, Balkan W, Reiner T, Perez-Stable C, et al. MutT Homolog 1
573 (MTH1) maintains multiple KRAS-driven pro-malignant pathways. *Oncogene*. 2015;34(20):2586-
574 2596.
- 575 26. Giribaldi MG, Munoz A, Halvorsen K, Patel A, Rai P. MTH1 expression is required for effective
576 transformation by oncogenic HRAS. *Oncotarget*. 2015;6(13):11519-11529.
- 577 27. Huber KV, Salah E, Radic B, Gridling M, Elkins JM, Stukalov A, et al. Stereospecific targeting of
578 MTH1 by (S)-crizotinib as an anticancer strategy. *Nature*. 2014;508(7495):222-227.
- 579 28. Nakabeppu Y. Cellular levels of 8-oxoguanine in either DNA or the nucleotide pool play pivotal
580 roles in carcinogenesis and survival of cancer cells. *Int J Mol Sci*. 2014;15(7):12543-12557.
- 581 29. Kettle JG, Alwan H, Bista M, Breed J, Davies NL, Eckersley K, et al. Potent and selective inhibitors
582 of MTH1 probe its role in cancer cell survival. *J Med Chem*. 2016;59(6):2346-2361.
- 583 30. Kawamura T, Kawatani M, Muroi M, Kondoh Y, Futamura Y, Aono H, et al. Proteomic profiling of
584 small-molecule inhibitors reveals dispensability of MTH1 for cancer cell survival. *Sci Rep*.
585 2016;6:26521.
- 586 31. Petrocchi A, Leo E, Reyna NJ, Hamilton MM, Shi X, Parker CA, et al. Identification of potent and
587 selective MTH1 inhibitors. *Bioorg Med Chem Lett*. 2016;26(6):1503-1507.
- 588 32. Samaranayake GJ, Huynh M, Rai P. MTH1 as a chemotherapeutic target: the elephant in the
589 room. *Cancers (Basel)*. 2017;9(5):47.
- 590 33. Coleman MP, Forman D, Bryant H, Butler J, Rachet B, Maringe C, et al. Cancer survival in
591 Australia, Canada, Denmark, Norway, Sweden, and the UK, 1995-2007 (the International Cancer
592 Benchmarking Partnership): an analysis of population-based cancer registry data. *Lancet*.
593 2011;377(9760):127-138.

- 594 34. Haslett K, Pottgen C, Stuschke M, Faivre-Finn C. Hyperfractionated and accelerated radiotherapy
1
2 595 in non-small cell lung cancer. *J Thorac Dis.* 2014;6(4):328-335.
3
4 596 35. Papeo G. MutT Homolog 1 (MTH1): The Silencing of a Target. *J Med Chem.* 2016;59(6):2343.
5
6 597 36. Singh NP, McCoy MT, Tice RR, Schneider EL. A simple technique for quantitation of low levels of
7
8 598 DNA damage in individual cells. *Exp Cell Res.* 1988;175(1):184-191.
9
10 599 37. Kelts JL, Cali JJ, Duellman SJ, Shultz J. Altered cytotoxicity of ROS-inducing compounds by sodium
11
12 600 pyruvate in cell culture medium depends on the location of ROS generation. *Springerplus.*
13
14 601 2015;4:269.
15
16 602 38. Warpman Berglund U, Sanjiv K, Gad H, Kalderen C, Koolmeister T, Pham T, et al. Validation and
17
18 603 development of MTH1 inhibitors for treatment of cancer. *Ann Oncol.* 2016;27(12):2275-2283.
19
20 604 39. Carter M, Jemth AS, Hagenkort A, Page BD, Gustafsson R, Griese JJ, et al. Crystal structure,
21
22 605 biochemical and cellular activities demonstrate separate functions of MTH1 and MTH2. *Nat*
23
24 606 *Commun.* 2015;6:7871.
25
26 607 40. Oka S, Ohno M, Tsuchimoto D, Sakumi K, Furuichi M, Nakabeppu Y. Two distinct pathways of cell
27
28 608 death triggered by oxidative damage to nuclear and mitochondrial DNAs. *EMBO J.* 2008;27(2):421-
29
30 609 432.
31
32 610 41. Yoshimura D, Salumi K, Ohio M, Sakai Y, Furuichi M, Iwata S, et al. An oxidized purine nucleoside
33
34 611 triphosphatase, MTH1, suppresses cell death caused by oxidative stress. *J Biol Chem.*
35
36 612 2003;278(39):37965-37973.
37
38 613 42. Haghdoost S, Czene S, Näslund I, Skog S, Harms-Ringdahl M. Extracellular 8-oxo-dG as a sensitive
39
40 614 parameter for oxidative stress in vivo and in vitro. *Free Radic Res.* 2005;39(2):153-162.
41
42 615 43. Ke Y, Lv Z, Yang X, Zhang J, Huang J, Wu S, et al. Compensatory effects of hOGG1 for hMTH1 in
43
44 616 oxidative DNA damage caused by hydrogen peroxide. *Toxicol Lett.* 2014;230(1):62-68.
45
46 617 44. Maréchal A, Zou L. DNA damage sensing by the ATM and ATR kinases. *Cold Spring Harbor*
47
48 618 *Perspect Biol.* 2013;5(9):a012716.
49
50
51
52
53
54
55
56
57
58
59
60
61
62
63
64
65

- 1
2
3
4
5
6
7
8
9
10
11
12
13
14
15
16
17
18
19
20
21
22
23
24
25
26
27
28
29
30
31
32
33
34
35
36
37
38
39
40
41
42
43
44
45
46
47
48
49
50
51
52
53
54
55
56
57
58
59
60
61
62
63
64
65
- 619 45. Britton S, Salles B, Calsou P. c-MYC protein is degraded in response to UV irradiation. *Cell Cycle*.
620 2008;7(1):63-70.
- 621 46. Conklin KA. Chemotherapy-associated oxidative stress: impact on chemotherapeutic
622 effectiveness. *Integr Cancer Ther*. 2004;3(4):294-300.
- 623 47. Donadelli M, Costanzo C, Beghelli S, Scupoli MT, Dandrea M, Bonora A, et al. Synergistic
624 inhibition of pancreatic adenocarcinoma cell growth by trichostatin A and gemcitabine. *Biochim*
625 *Biophys Acta*. 2007;1773(7):1095-1106.
- 626 48. Oguri T, Achiwa H, Sato S, Bessho Y, Takano Y, Miyazaki M, et al. The determinants of sensitivity
627 and acquired resistance to gemcitabine differ in non-small cell lung cancer: a role of ABCC5 in
628 gemcitabine sensitivity. *Mol Cancer Ther*. 2006;5(7):1800-1806.
- 629 49. Bepler G, Kusmartseva I, Sharma S, Gautam A, Cantor A, Sharma A, et al. RRM1 modulated in
630 vitro and in vivo efficacy of gemcitabine and platinum in non-small-cell lung cancer. *J Clin Oncol*.
631 2006;24(29):4731-4737.
- 632 50. Toschi L, Cappuzzo F. Gemcitabine for the treatment of advanced nonsmall cell lung cancer.
633 *Onco Targets Ther*. 2009;2:209-217.
- 634 51. Basu A, Krishnamurthy S. Cellular responses to cisplatin-induced DNA damage. *J Nucleic Acids*.
635 2010; doi:10.4061/2010/201367.
- 636 52. Un F. G1 arrest induction represents a critical determinant for cisplatin cytotoxicity in G1
637 checkpoint-retaining human cancers. *Anticancer Drugs*. 2007;18(4):411-417.
- 638 53. Itoh T, Terazawa R, Kojima K, Nakane K, Deguchi T, Ando M, et al. Cisplatin induces production of
639 reactive oxygen species via NADPH oxidase activation in human prostate cancer cells. *Free Radic Res*.
640 2011;45(9):1033-1039.
- 641 54. Casares C, Ramirez-Camacho R, Trinidad A, Roldan A, Jorge E, Garcia-Berrocal JR. Reactive oxygen
642 species in apoptosis induced by cisplatin: review of physiopathological mechanisms in animal
643 models. *Eur Arch Otorhinolaryngol*. 2012;269(12):2455-2459.

- 644 55. Marullo R, Werner E, Degtyareva N, Moore B, Altavilla G, Ramalingam SS, et al. Cisplatin induces
1
2 645 a mitochondrial-ROS response that contributes to cytotoxicity depending on mitochondrial redox
3
4 646 status and bioenergetic functions. *PLoS One*. 2013;8(11):e81162.
5
6
7 647 56. Wikman H, Risch A, Klimek F, Schmezer P, Spiegelhalder B, Dienemann H, et al. hOGG1
8
9 648 polymorphism and loss of heterozygosity (LOH): significance for lung cancer susceptibility in a
10
11 649 caucasian population. *Int J Cancer*. 2000;88(6):932-937.
12
13
14 650 57. Mambo E, Chatterjee A, de Souza-Pinto NC, Mayard S, Hogue BA, Hoque MO, Dizdaroglu M, et al.
15
16 651 Oxidized guanine lesions and hOgg1 activity in lung cancer. *Oncogene*. 2005;24(28):4496-4508.
17
18
19 652 58. Long LH, Halliwell B. Artefacts in cell culture: pyruvate as a scavenger of hydrogen peroxide
20
21 653 generated by ascorbate or epigallocatechin gallate in cell culture media. *Biochem Biophys Res*
22
23 654 *Commun*. 2009;388(4):700-704.
24
25
26 655 59. Fotouhi A, Skiold S, Shakeri-Manesh S, Osterman-Golkar S, Wojcik A, Jenssen D, et al. Reduction
27
28 656 of 8-oxodGTP in the nucleotide pool by hMTH1 leads to reduction in mutations in the human
29
30 657 lymphoblastoid cell line TK6 exposed to UVA. *Mutat Res*. 2011;715(1-2):13-18.
31
32
33 658 60. Russo MT, Blasi MF, Chiera F, Fortini P, Degan P, Macpherson P, et al. The oxidized
34
35 659 deoxynucleoside triphosphate pool is a significant contributor to genetic instability in mismatch
36
37 660 repair-deficient cells. *Mol Cell Biol*. 2004;24(1):465-474.
38
39
40 661 61. Mazouzi A, Velimezi G, Loizou JI. DNA replication stress: causes, resolution and disease. *Exp Cell*
41
42 662 *Res*. 2014;329(1):85-93.
43
44
45 663 62. Zeman MK, Cimprich KA. Causes and consequences of replication stress. *Nat Cell Biol*.
46
47 664 2014;16(1):2-9.
48
49
50 665 63. Strumberg D, Pilon AA, Smith M, Hickey R, Malkas L, Pommier Y. Conversion of Topoisomerase I
51
52 666 Cleavage Complexes on the Leading Strand of Ribosomal DNA into 59-Phosphorylated DNA Double-
53
54 667 Strand Breaks by Replication Runoff. *Mol Cell Biol*. 2000;20(11):3977-3987.
55
56
57
58
59
60
61
62
63
64
65

- 668 64. Hanada K, Budzowska M, Davies SL, van Drunen E, Onizawa H, Beverloo HB, et al. The structure-
1
2 669 specific endonuclease Mus81 contributes to replication restart by generating double-strand DNA
3
4 670 breaks. *Nat Struct Mol Biol.* 2007;14(11):1096-1104.
5
6
7 671 65. Regairaz M, Zhang Y, Fu H, Agama KK, Tata N, Agrawal S, et al. Mus81-mediated DNA cleavage
8
9 672 resolves replication forks stalled by topoisomerase I-DNA complexes. *J Cell Biol.* 2011;195(5):739-
10
11 673 749.
12
13
14 674 66. Lee JA, Carvalho CMB, Lupski JR. A DNA Replication Mechanism for Generating Nonrecurrent
15
16 675 Rearrangements Associated with Genomic Disorders. *Cell.* 2007;131(7):1235-1247.
17
18
19 676 67. Zhang F, Towne CF, Lupski JR, Connolly AM, Khajavi M, Batish SD. The DNA replication
20
21 677 FoSTeS/MMBIR mechanism can generate genomic, genic and exonic complex rearrangements in
22
23 678 humans. *Nature Genet.* 2009;41(7):849-853.
24
25
26 679 68. Hastings PJ, Ira G, Lupski JR. A microhomology-mediated break-induced replication model for the
27
28 680 origin of human copy number variation. *PLoS Genet.* 2009;5(1):e1000327.
29
30
31 681 69. Liu P, Erez A, Nagamani S, Dhar S, Kołodziejaska K, Dharmadhikari A, et al. Chromosome
32
33 682 catastrophes involve replication mechanisms generating complex genomic rearrangements. *Cell.*
34
35 683 2011;146(6):889-903.
36
37
38 684 70. Shiotani B, Zou L. Single-stranded DNA orchestrates an ATM-to-ATR switch at DNA breaks. *Mol*
39
40 685 *Cell.* 2009;33(5):547-558.
41
42
43 686 71. Merry C, Fu K, Wang J, Yeh I, Zhang Y. Targeting the checkpoint kinase Chk1 in cancer therapy.
44
45 687 *Cell Cycle.* 2010;9(2):279-283.
46
47
48 688 72. Zhang Y, Hunter T. Roles of Chk1 in cell biology and cancer therapy. *Int J Cancer.*
49
50 689 2014;134(5):1013-1023.
51
52 690 73. Wang JY, Jin L, Yan XG, Sherwin S, Farrelly M, Zhang YY, et al. Reactive oxygen species dictate the
53
54 691 apoptotic response of melanoma cells to TH588. *J Invest Dermatol.* 2016;136(11):2277-2286.
55
56
57 692
58
59 693
60
61
62
63
64
65

694 **Figure Legends**

1
2 695 **Fig. 1** MTH1 is efficiently knocked down in various lung cancer cell lines and normal lung fibroblasts.
3
4 696 Western blots to determine MTH1 protein levels in cell cultures grown in media without transfection
5
6 697 reagent (no siRNA), or following transfection with MTH1 siRNA or scramble siRNA. **a** H23. **b** A549. **c**
8
9 698 H522. **d** MRC-5. Representative day 4 blots shown. Day 4 MTH1 band intensities were normalized to
10
11 699 corresponding α -Tubulin loading control bands, and then siRNA samples were normalised to
12
13 700 corresponding no siRNA bands. Numbers of independent experiments (n) are indicated. Mean values
14
15 701 and SD were calculated from the normalised values of the independent experiments. Error bars
16
17 702 represent SD. Asterisks represent a significant difference between MTH1 siRNA and corresponding
18
19 703 no siRNA normalised values (****P<0.0001, *P<0.05).
20
21 704

25 705 **Fig. 2** MTH1 knockdown leads to increased oxidised DNA base levels in lung cancer cell genomes.
26
27 706 Formamidopyrimidine-DNA glycosylase (Fpg)-modified alkaline comet assay to determine DNA
28
29 707 damage levels (expressed as % tail DNA) in individual cells grown in media without transfection
30
31 708 reagent (no siRNA), or 4 days after transfection with MTH1 siRNA or scramble siRNA. DNA single-
32
33 709 strand breaks detected as Fpg-independent signal, while oxidatively damaged DNA bases detected
34
35 710 by treatment with Fpg. **a** H23, 8 independent experiments. **b** A549, 3 independent experiments. **c**
36
37 711 H522, 4 independent experiments. **d** MRC-5, 3 independent experiments. For **(a)** to **(d)**, 200
38
39 712 randomly selected individual comets were scored for each sample per experiment. Mean values
40
41 713 from independent experiments were used to generate final mean values and SD. Error bars
42
43 714 represent SD. Asterisks indicate a significant difference between Fpg-treated MTH1 siRNA and
44
45 715 scramble siRNA experiment means (****P<0.0001, ***P<0.001, *P<0.05); ns, not significant. **e**
46
47 716 Internal ROS levels determined by measuring fluorescence signal induced by 2',7'-
48
49 717 dichlorodihydrofluorescein diacetate oxidisation. RFU, relative fluorescence units. Blank samples
50
51 718 were without seeded cells. Mean values were calculated from 4 independent experiments. Error
52
53 719 bars represent SD calculated from the independent experiment values. Unpaired T-test was
54
55
56
57
58
59
60
61
62
63
64
65

720 performed. Asterisks indicate a significant difference between hydrogen peroxide treated and
721 untreated samples (***P<0.001, **P<0.01 and *P<0.05). **f** Comet assay post-irradiation of H23 cells.
722 Error bars represent SEM calculated from 400 individual comet values analysed in total from 2
723 independent experiments. No statistical analysis was performed.

724

Fig. 3 Alterations in DNA damage response signalling following MTH1 knockdown. Cells were grown
725 in media without transfection reagent (no siRNA), or transfected with MTH1 siRNA or scramble
726 siRNA (Scr. siRNA). Western blots were performed 4 days post-transfection. Positive control samples
727 (+ve) were H23 cells treated with VP-16 (etoposide, 25 µg/ml), phleomycin (25 µg/ml) or
728 hydroxyurea (2 mM) for 2 hours. **a** and **c** Representative Western blots. **b** pChk2(Thr68) band
729 intensities from H522 samples were normalised to α-Tubulin, and expression levels calculated
730 relative to no siRNA samples. **d** Chk1 Western blot band intensities were normalized to α-Tubulin,
731 and expression levels calculated relative to no siRNA samples. Mean values and SD were calculated
732 from the normalised values of the 3 independent experiments. Error bars represent SD. Asterisks
733 represent a significant difference between MTH1 siRNA and no siRNA normalised values
734 (****P<0.0001).

736

Fig. 4 MTH1 targeting reduces H23 cell proliferative capacity. WST-1 assay on cells grown in media
737 without transfection reagent (no siRNA), or 5 days after transfection with MTH1 siRNA or scramble
738 siRNA. **a** H23. **b** A459. **c** H522. **d** MRC-5. (**a**), (**b**) and (**d**) Values from 4 independent experiments were
739 used to generate final mean values and SD. (**c**) Values from 3 independent experiments were used to
740 generate final mean values and SD. Error bars represent SD. Asterisks indicate a significant
741 difference relative to corresponding no siRNA controls (****P<0.0001, ***P<0.001, **P<0.01,
742 *P<0.05).

744

1
2
3
4
5
6
7
8
9
10
11
12
13
14
15
16
17
18
19
20
21
22
23
24
25
26
27
28
29
30
31
32
33
34
35
36
37
38
39
40
41
42
43
44
45
46
47
48
49
50
51
52
53
54
55
56
57
58
59
60
61
62
63
64
65

Fig. 5 MTH1 deficiency does not induce apoptosis or augment the cytotoxic effects of chemotherapy agents. Apoptosis assay to determine viability of cells cultured for 4 days in media without transfection reagent (no siRNA), or following transfection with MTH1 siRNA or scramble siRNA. Positive control of 48 hours VP-16 treatment (+ve) also included. Harvested cells were dual stained with annexin V-FITC/propidium iodide (PI) and assessed by flow cytometry. Annexin V is an apoptosis marker. PI is a DNA stain that is excluded from viable and early apoptotic cells. Percentage values from independent experiments were used to calculate final mean values and SD. Error bars represent SD. **a** Representative bivariate plots of H23 cells. **b** H23. **c** A549. **d** H522. **e** MRC-5. (**b**) and (**c**) 3 independent experiments performed. (**d**) and (**e**) 4 independent experiments performed. Asterisks indicate a significant difference relative to corresponding no siRNA control (or no siRNA + DMSO control in case of VP-16). **f** H23 cells. 2 days after transfection, 0.01 μ M gemcitabine (Gem) or 5 μ M cisplatin (Cis) were added to the appropriate cultures for the remaining 48 hours (0.5% DMSO). 3 independent experiments performed with siRNA transfections (5 repeats for non-transfected samples). **g** H522 cell line. 2 days after transfection, 40 μ M gemcitabine (Gem) or 10 μ M cisplatin (Cis) were added to the appropriate cultures for the remaining 48 hours (1.5% DMSO). 3 independent experiments performed with siRNA transfections and Cis and Gem treatments (4 repeats for untreated and non-transfected samples). (**f**) and (**g**) Asterisks in Scramble siRNA and MTH1 siRNA samples indicate a significant difference between No treatment, Gem or Cis and corresponding no siRNA + DMSO, no siRNA + Gem and no siRNA + Cis percentage values, respectively (**** $P < 0.0001$, ** $P < 0.01$, * $P < 0.05$).

Fig. 6 Variable effects of TH287 and TH588 MTH1 inhibitors on DNA oxidation and apoptosis. **a** to **d** Fpg-modified alkaline comet assay. DMSO (0.066 % v/v) used as a vehicle control. Means \pm SD calculated from 3 independent experiments. 200 randomly selected individual comets were scored for each sample per experiment. Mean values calculated from 3 independent experiments were used to generate final mean values and SD. Error bars represent SD. **e** to **h** Annexin V-FITC/PI

1 771 apoptosis assay to determine cell viability. DMSO (0.5-1.5% v/v) or VP-16 (+ve) were applied as
2 772 vehicle controls and positive controls, respectively. 3 independent experiments performed (except
3
4 773 150 μ M VP-16). Percentage values from each experiment were used to calculate final mean values
5
6
7 774 and SD. Error bars represent SD. Asterisks indicate a significant difference between treated and
8
9 775 untreated percentage values (****P<0.0001, **P<0.01, *P<0.05).

10
11 776

12
13
14 777 **Additional files**

15
16 778 **Additional file 1** Endogenous MTH1 levels are similar in H23, H522, A549 and MRC-5 cell lines. MTH1
17
18
19 779 band intensities in no siRNA samples were normalized to corresponding α -Tubulin loading control
20
21 780 bands (see Figure 1 for representative Western blot images). Mean values and SD were calculated
22
23 781 from the normalised values of independent experiments. Numbers of independent experiments (n)
24
25
26 782 are indicated. Error bars represent SD.

27
28 783

29
30 784 **Additional file 2** MTH2 levels are stable following MTH1 siRNA knockdown. Western blots from a
31
32
33 785 single confirmation experiment performed to determine MTH2 protein levels in cell cultures grown
34
35 786 in media without transfection reagent (no siRNA), or following transfection with MTH1 siRNA or
36
37 787 scramble siRNA (n = 1).

38
39
40 788

41
42 789 **Additional file 3** Representative images of “Comets” and the corresponding intensity profiles,
43
44
45 790 showing (i) ~5% Tail DNA damage, typical of the NSCLC cells treated with no siRNA or scramble
46
47 791 siRNA, and analysed by regular Fpg-modified alkaline comet assay (0.8U Fpg/gel); and (ii) comets
48
49 792 showing ~10% tail DNA, typical of the NSCLC cells treated with MTH1 siRNA. Superimposed on the
50
51
52 793 Comet images are the image analysis software (Komet 5.5, Andor Technology) determined
53
54 794 boundaries demarcating the ‘Comet head’ (pink circle) and ‘tail extent’ (vertical orange line) (Barber
55
56 795 RC, Hickenbotham P, Hatch T, Kelly D, Topchiy N, Almeida GM, et al. Radiation-induced
57
58 796 transgenerational alterations in genome stability and DNA damage. *Oncogene*. 2006;25(56):7336-

797 7342). % tail DNA = 100 - % head DNA; % head DNA = (integrated optical head intensity / (integrated
1
2 798 optical head intensity + integrated optical tail intensity)) x 100.
3

4
5 799

6
7 800 **Additional file 4** MTH1 deficiency does not alter levels of oxidatively-modified DNA following
8
9 801 hydrogen peroxide treatment. Fpg-modified alkaline comet assay to determine DNA damage levels
10
11 802 in individual cells grown in media without transfection reagent (no siRNA), or 4 days after
12
13 803 transfection with MTH1 siRNA or scramble siRNA. After 30 minutes hydrogen peroxide treatment at
14
15 804 37°C, samples were collected either immediately or allowed to recover in fresh media. Means were
16
17 805 calculated from 100 individual comets from a single experiment. Error bars represent SEM of comet
18
19 806 values. **a** H23. **b** H522.
20
21

22
23 807

24
25
26 808 **Additional file 5** MTH1 knockdown with another siRNA similarly does not induce apoptosis in H23
27
28 809 cells. **a** Western blots to determine MTH1 protein levels in H23 cell cultures grown in media without
29
30 810 transfection reagent (no siRNA), or following transfection with MTH1 siRNA (ThermoFisher Scientific,
31
32 811 S194633, oligonucleotide 5'->3' sequences were sense UUAACUGGAUGGAAGGGAAtt and antisense
33
34 812 AUCCAGUUAUCCAGAUGaa) or scramble siRNA. Representative day 4 blot shown. Day 4 MTH1
35
36 813 band intensities were normalized to corresponding α -Tubulin loading control bands, and then siRNA
37
38 814 samples were normalised to corresponding no siRNA bands. Numbers of independent experiments
39
40 815 (n) are indicated. Mean values were calculated from the normalised values of the independent
41
42 816 experiments. Error bars represent SD. Asterisks represent a significant difference between MTH1
43
44 817 siRNA and corresponding no siRNA normalised values (**P<0.01, *P<0.05). **b** Apoptosis assay to
45
46 818 determine cell viability of H23 cells cultured for 4 days in media without transfection reagent (no
47
48 819 siRNA), or following transfection with MTH1 siRNA (S194633) or scramble siRNA. Harvested cells
49
50 820 were dual stained with annexin V-FITC/PI and assessed by flow cytometry to detect both early and
51
52 821 late apoptosis. 2 days after transfection, 0.01 μ M gemcitabine (Gem) or 5 μ M cisplatin (Cis) were
53
54
55
56
57
58
59
60
61
62
63
64
65

1 822 added to the appropriate cultures for the remaining 48 hours. Positive control of 48 hours VP-16
2 823 treatment (+ve) also included (n = 1).
3

4 824
5

6
7 825 **Additional file 6** Apoptotic dose responses of H23 and H522 cell lines to various genotoxic agents.
8
9 826 Apoptosis assay to determine cell viability following 48 hours treatment with different agents. In
10
11 827 addition, cells were exposed to VP-16 for positive controls, and DMSO (0.5-2% v/v) and untreated
12
13 828 negative control samples were also included. Harvested cells were dual stained with annexin V-
14
15 829 FITC/PI and assessed by flow cytometry to detect both early and late apoptosis. **a** Hydrogen peroxide
16
17 830 treatment of H23 and H522 cells. **b** Gemcitabine treatment of H2 and H522 cells. **c** Cisplatin
18
19 831 treatment of H2 and H522 cells. Percentage values from independent experiments were used to
20
21 832 calculate final mean values and SD. Error bars represent SD. All experiments were repeated more
22
23 833 than 3 times. Asterisks indicate a significant difference relative to corresponding DMSO controls
24
25 834 (****P<0.0001, ***P<0.001, **P<0.01, and *P<0.05).
26
27
28
29
30
31
32
33
34
35
36
37
38
39
40
41
42
43
44
45
46
47
48
49
50
51
52
53
54
55
56
57
58
59
60
61
62
63
64
65

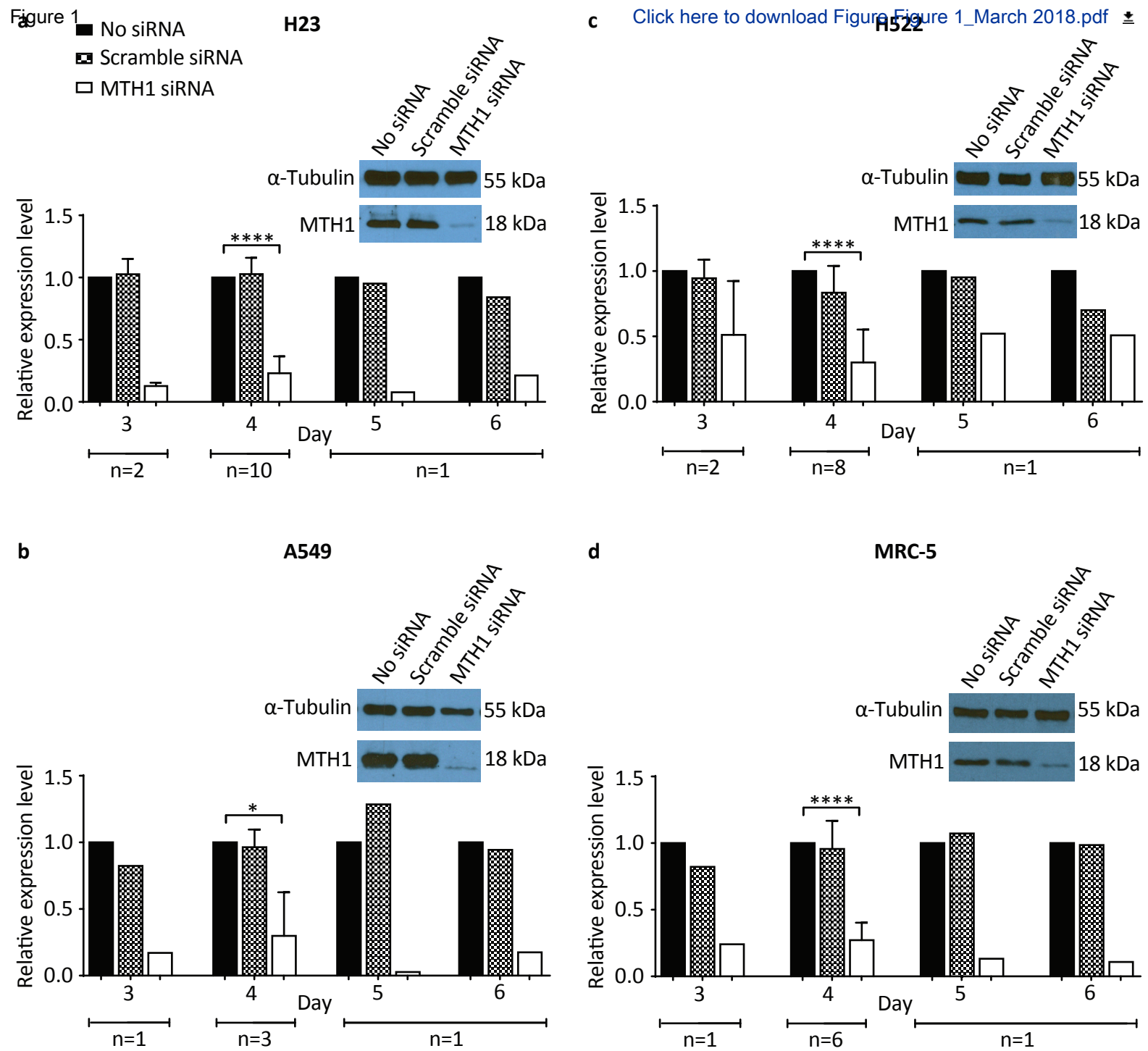
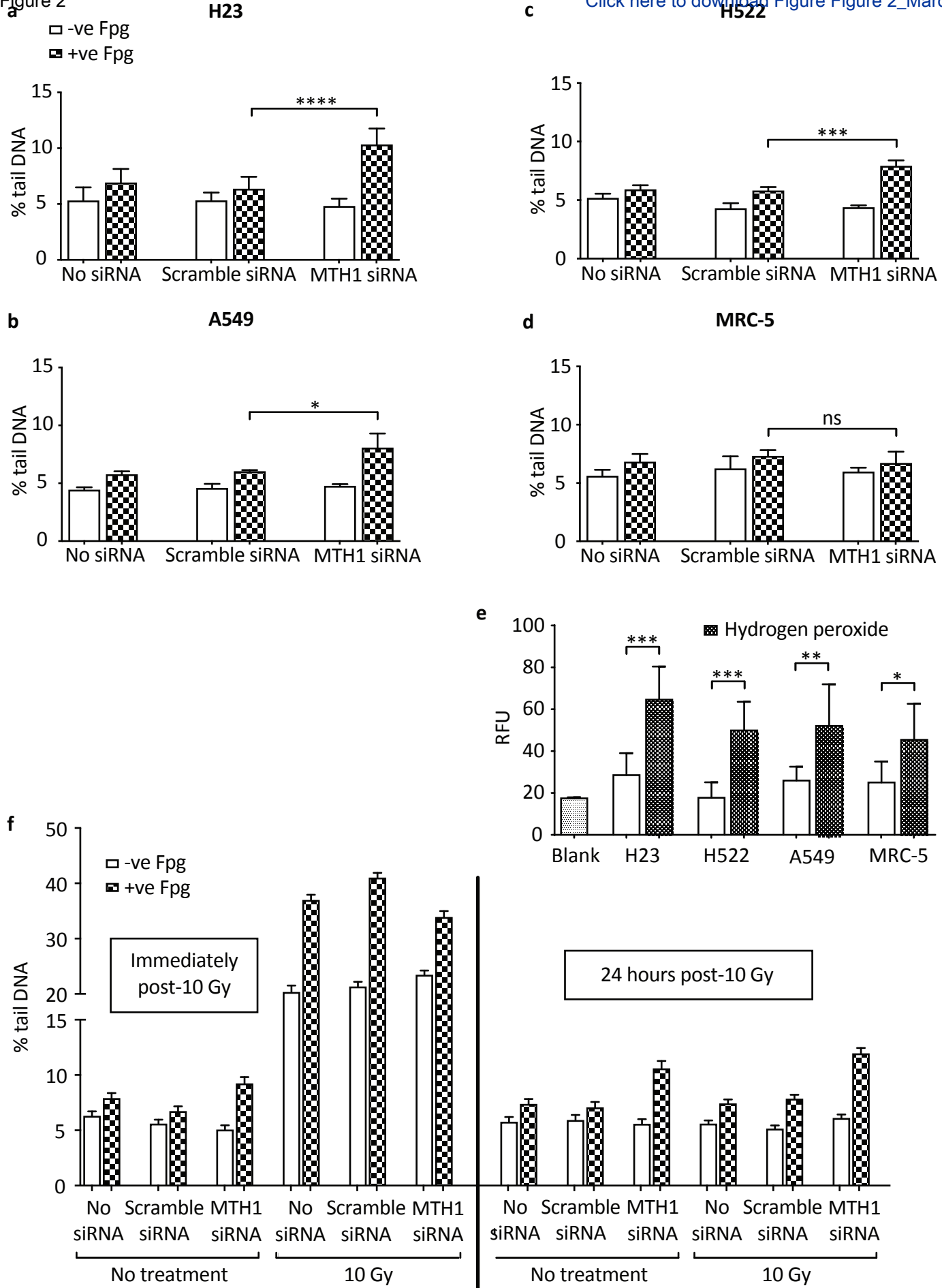
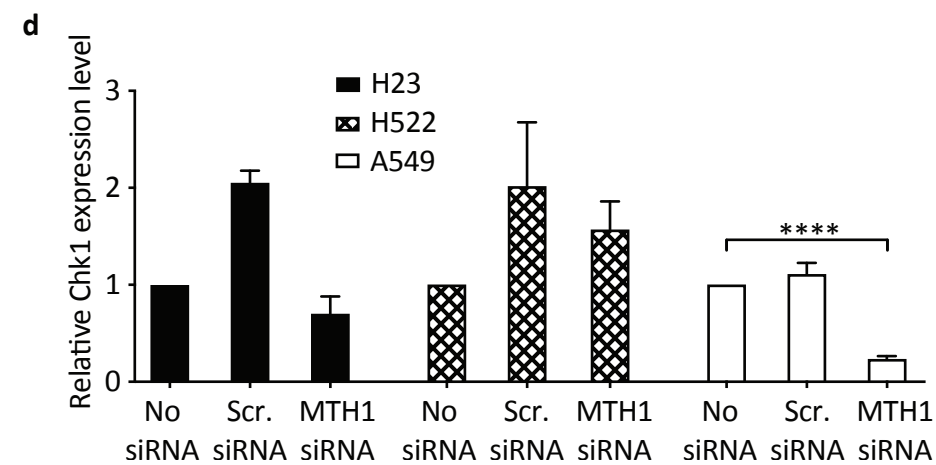
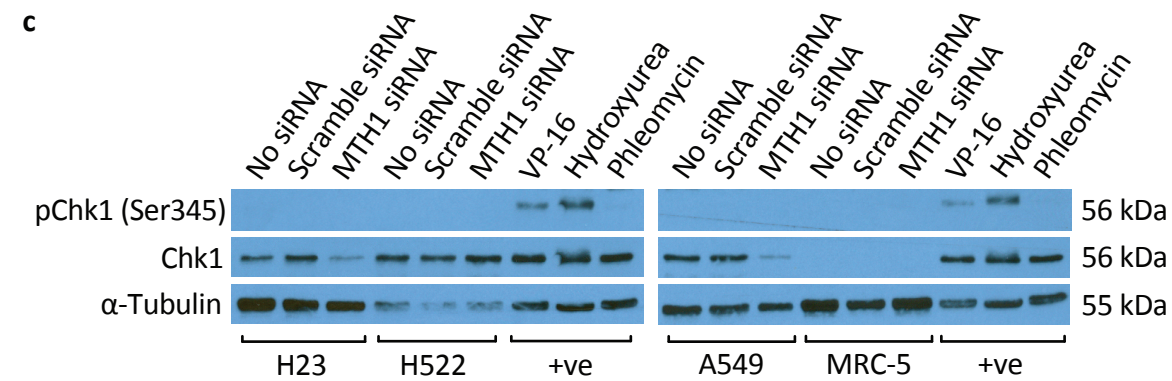
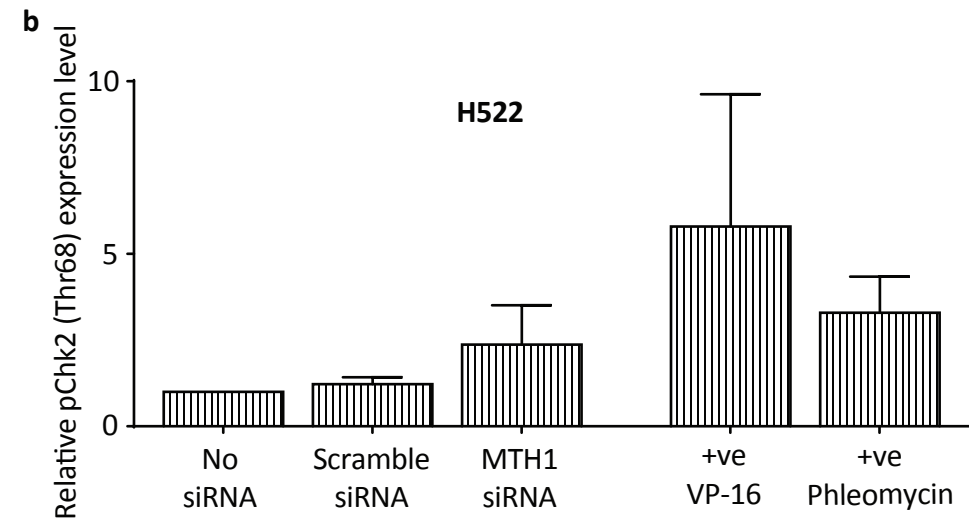
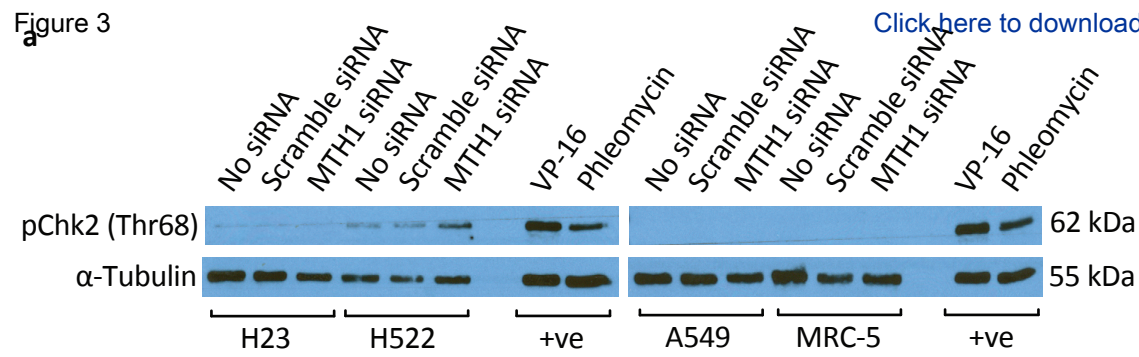


Figure 2





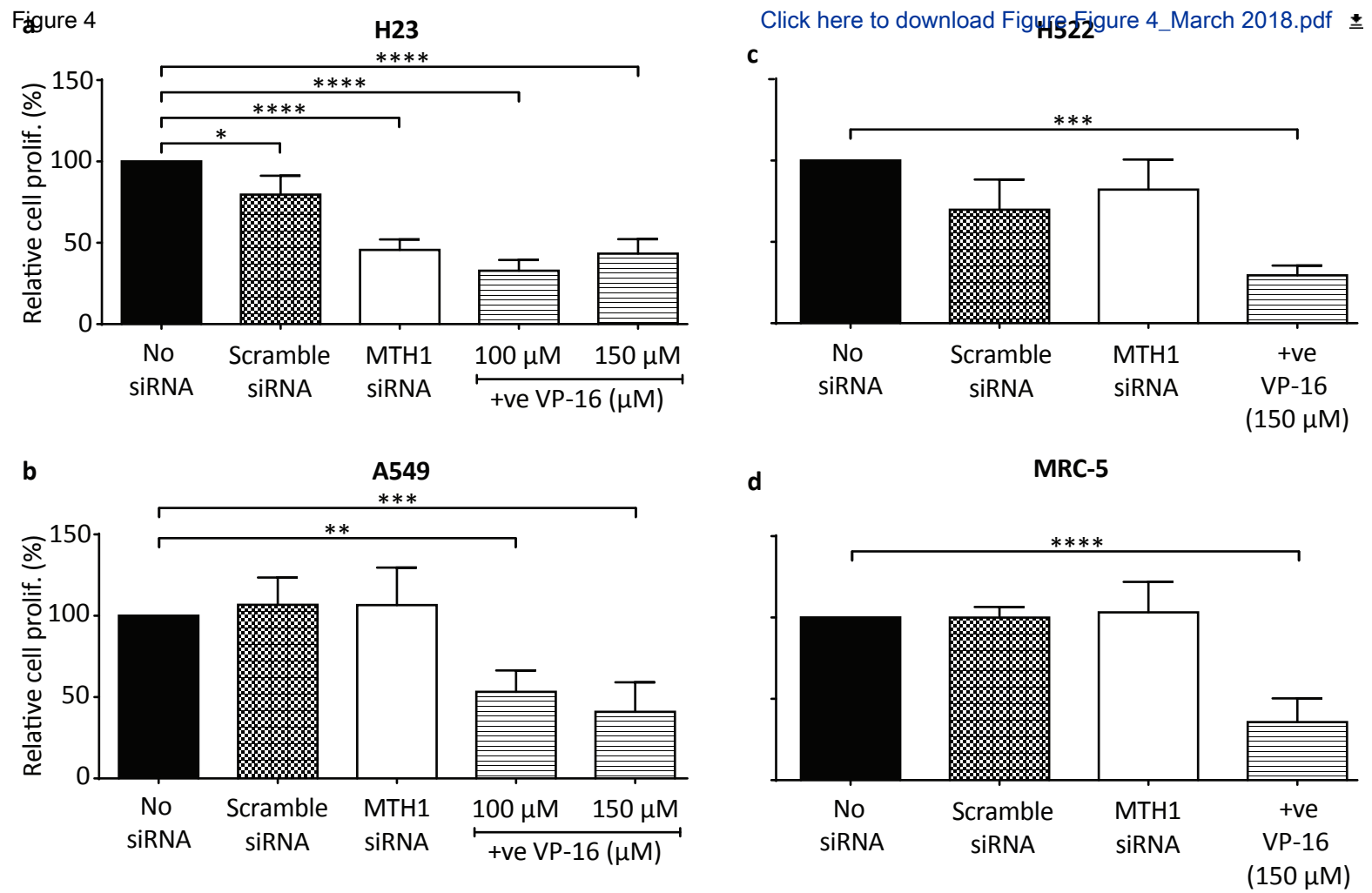


Figure 5

[Click here to download Figure Figure 5_March 2018.pdf](#)

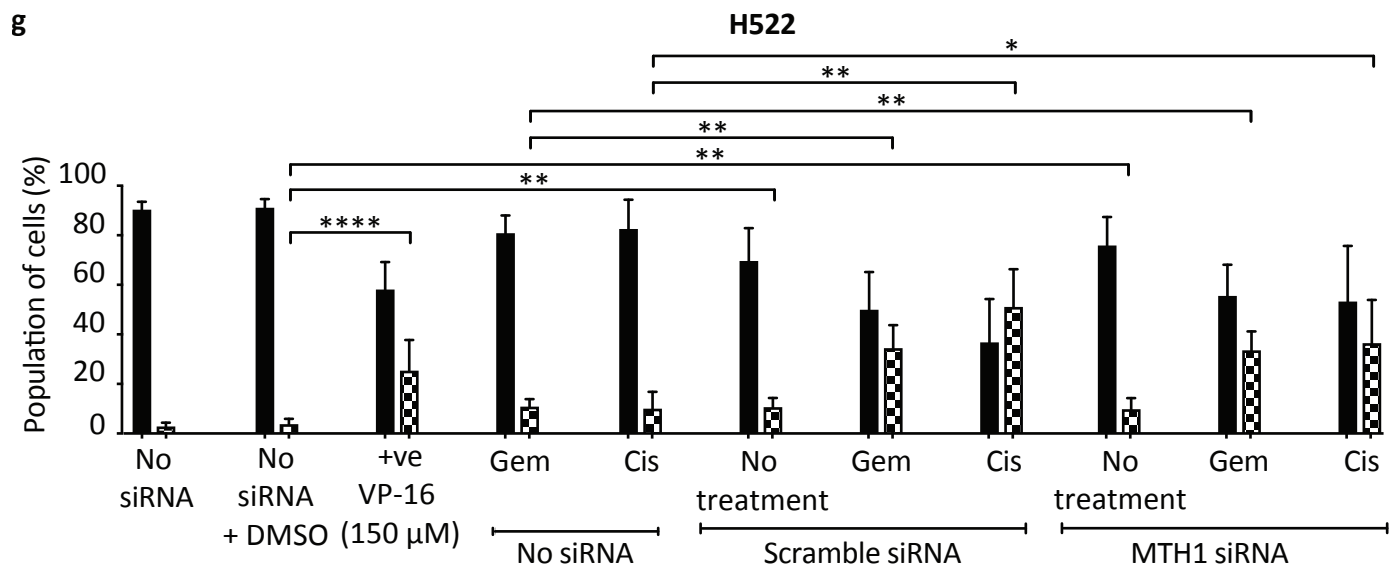
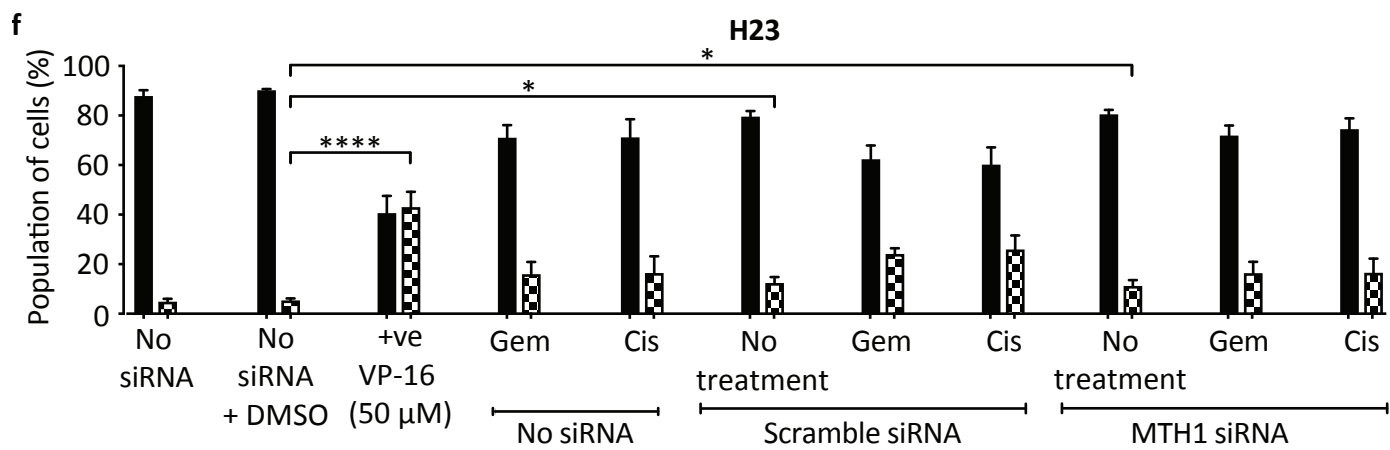
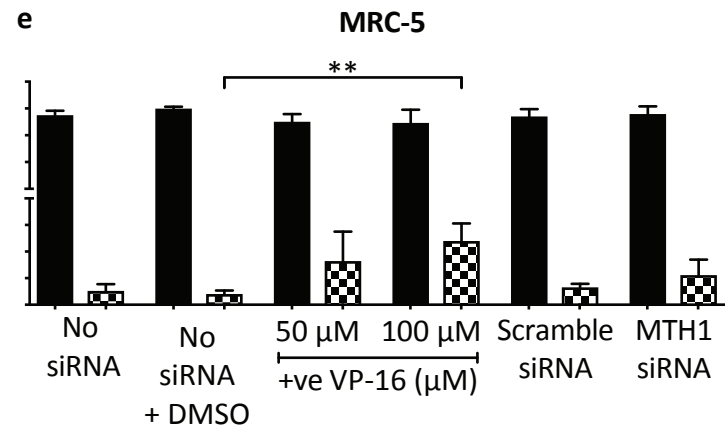
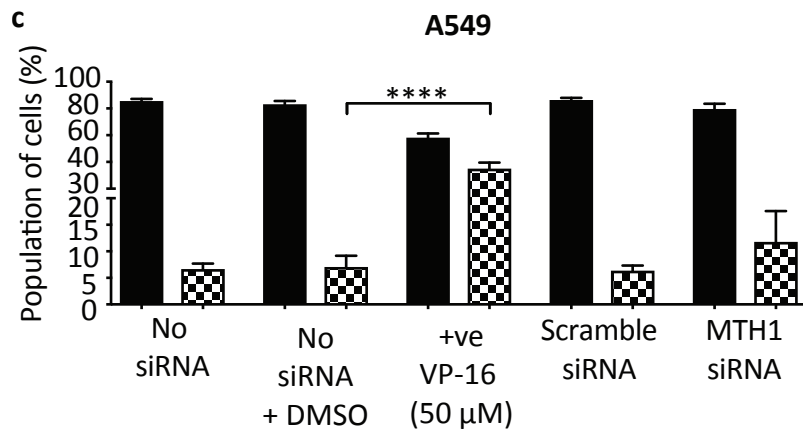
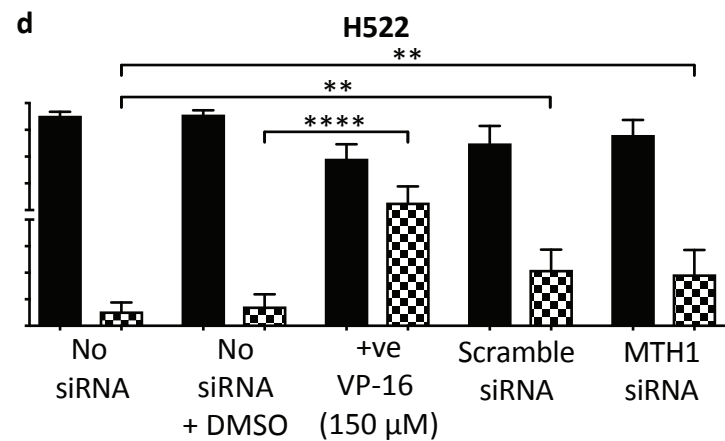
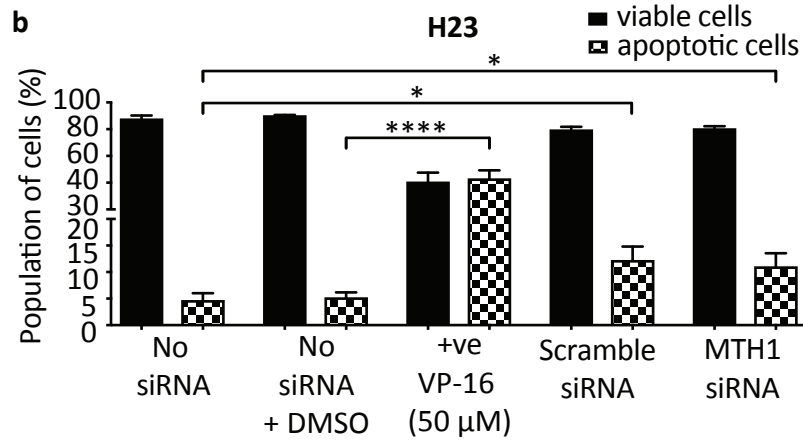
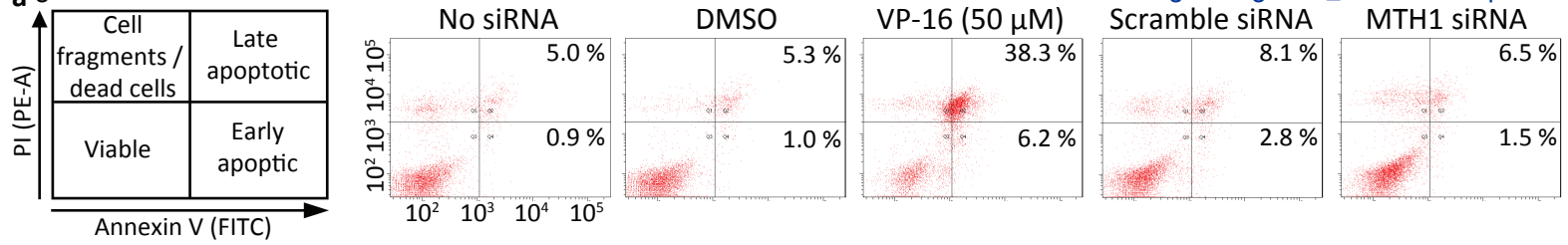
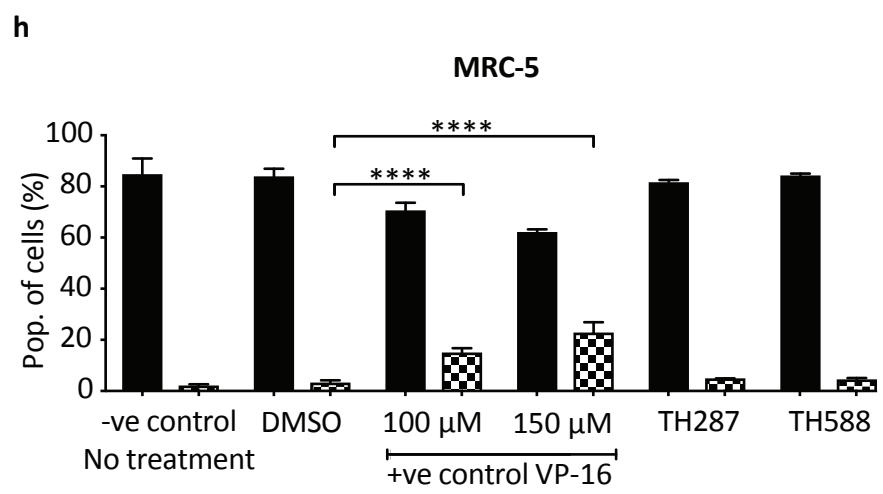
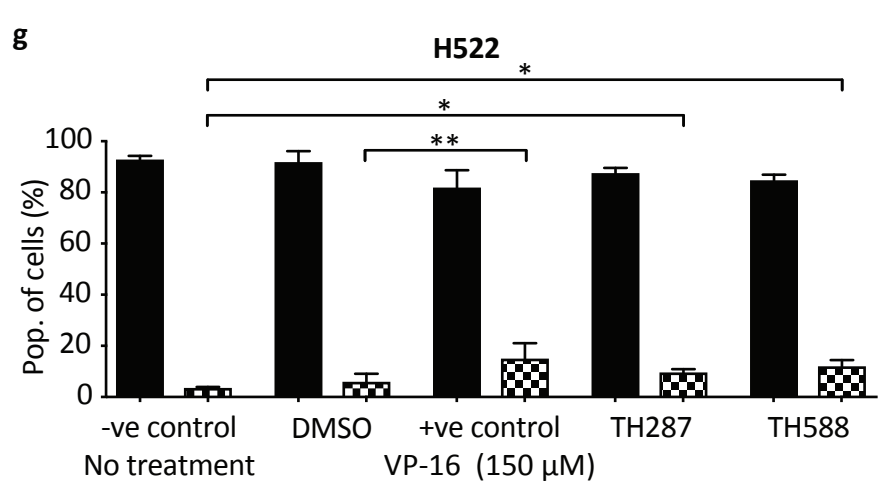
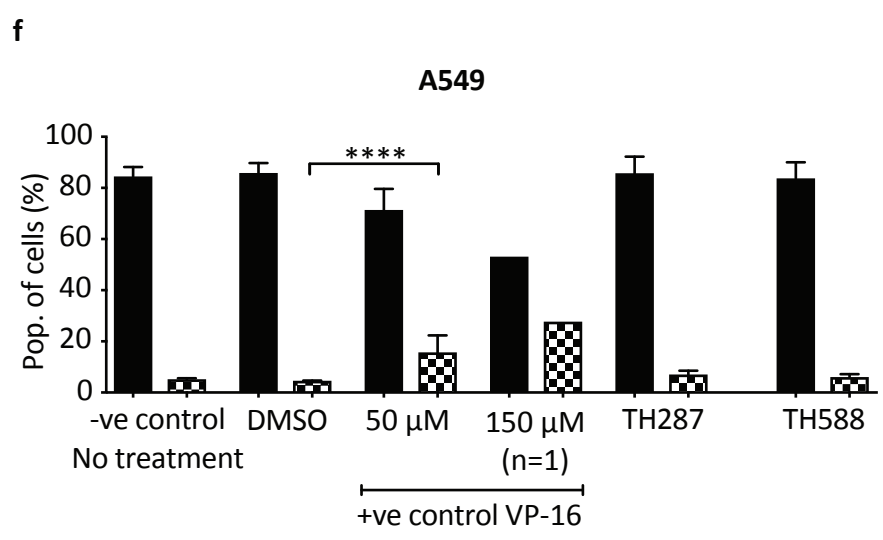
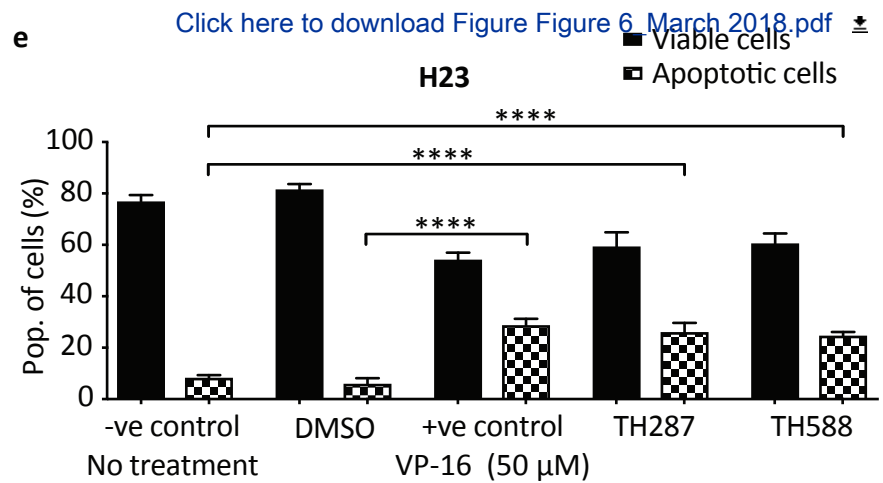
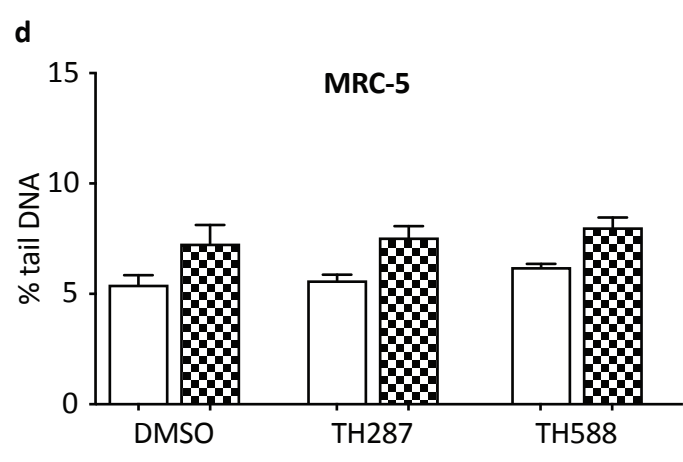
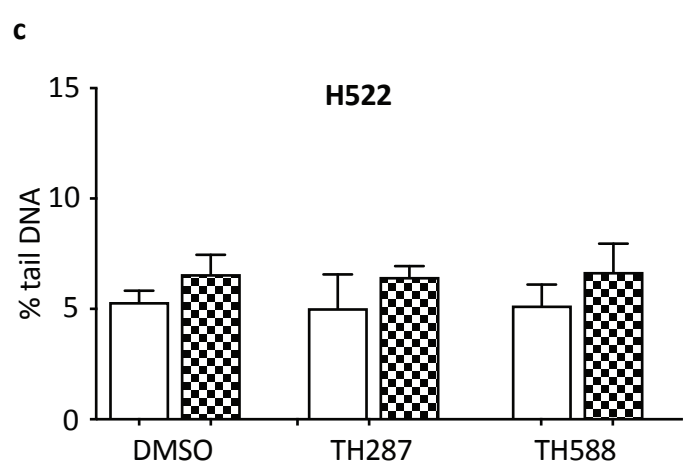
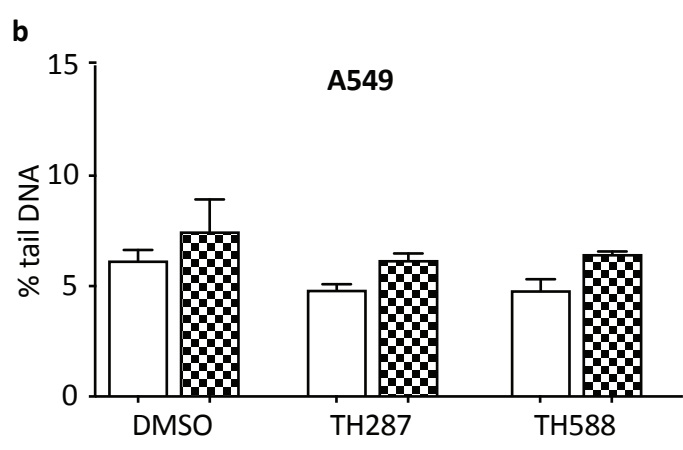
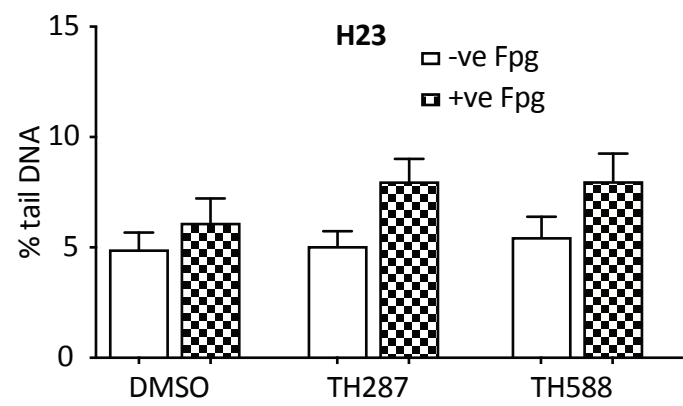


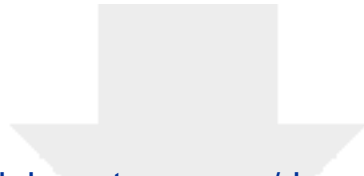
Figure 6



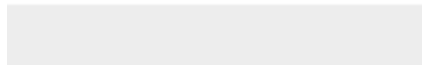
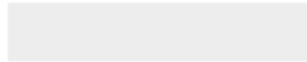


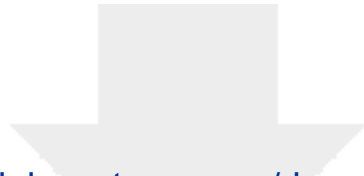
Click here to access/download
Supplementary Material
Additional file 1_March 2018.pdf



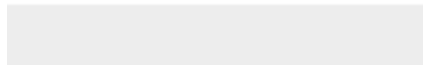


Click here to access/download
Supplementary Material
Additional file 2_March 2018.pdf





Click here to access/download
Supplementary Material
Additional file 3_March 2018.pdf





Click here to access/download
Supplementary Material
Additional file 4_March 2018.pdf





Click here to access/download
Supplementary Material
Additional file 5_March 2018.pdf





Click here to access/download
Supplementary Material
Additional file 6_March 2018.pdf

